



# KONKAN GYANPEETH COLLEGE OF ENGINEERING KARJAT

(Approved by A.I.C.T.E. - New Delhi & DTE Govt. of Maharashtra State,  
Affiliated to University of Mumbai)

Konkan Gyanpeeth Shikshank Sankul, At. Vengalim Road, Dahival / Parade,  
Post - Thane, Tal - Karjat, Dist Raigad 410201 M S (India)

Tel : (02148) 22 25 80 / 22 37 88

Email: kgce@vsnl.net, kgce2009@gmail.com website: www.kgce.edu.in

Dr. Anurag Dinkar Wagh  
Chairperson

Dr. Sanku Wagh  
Vice Chairman

Dr. P. V. Shringarpure  
Secretary & CEO

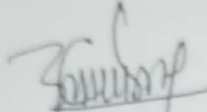
Dr. Z. A. Dabhiya  
Treasurer

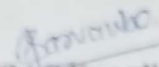
Dr. M. J. Lengare  
Principal

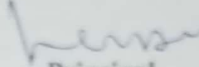
KGCE/AQAR 2018-19/Cr-3

Date: 28/11/2019

Criteria: 3.3.3	Research Publications in the Journals notified on UGC website during the year
Response	1. List of Research Publications in the Journals notified on UGC website 2. List of documents ( <i>Appendix-I</i> )

  
Cr-3 Co-ordinator  
Prof.R.P.Narkhede

  
IQAC Co-ordinator  
Prof.G.S.Darvankar

  
Principal  
Dr.M.J.Lengare





**KONKAN GYANPEETH  
COLLEGE OF ENGINEERING KARJAT**

(Approved by A.I.C.T.E. - New Delhi & DTE Govt. of Maharashtra State,  
Affiliated to University of Mumbai)

Konkan Gyanpeeth Shaikshanik Sankul, At. Vengason Road, Dahivali / Parade,  
Post - Tiwari, Tal - Karjat, Dist. Raigad 410201 M.S (India)

Tel : (02148) 22 25 80 / 22 37 68

Email : kgce@vsnl.net, kgce2009@gmail.com website : www.kgce.edu.in

Smt. Anupama Dharkar Wangdi  
Chairperson

Capt. Saripuffa Wangdi  
Vice Chairman

Shri P. V. Shringarpure  
Secretary & CEO

Shri. Z. A. Dabhiya  
Treasurer

Dr. M. J. Lengare  
Principal

Date: 28/11/2019

3.3.3 Research Publications in the Journals notified on UGC website during the year

Sr. No.	Type	Name of Faculty	Department	Title of the Paper	Publisher	No. of Publication	Average Impact Factor, if any
1	National				NIL		
<b>International</b>							
1	International	Dr. V.J. Pillewan	MECH	Carbon to Carbon Nanotubes Synthesis Process: An experimental and numerical study	ELSEVIER Science Direct, Materials Today: Proceedings, Volume 5, Issue 2(1), 2018, Page No. 6444-6452.	1	3.481
2	International	Dr. V.J. Pillewan	MECH	Wear Analysis of Charcoal, unprufied nanotubes and purified corbon nanotubes based metal matrix composite	ELSEVIER Science Direct, Materials Today: Proceedings, Voi. 5, 2018, Page No. 20679-20689.	1	3.481
3	International	Prof. R.S. Meshram, Mr. Hitesh Bhoir, Mr. Rakesh Pawar	EXTC	Car locking and tracking	IJARIE, Paper ID 10034, e-ISSN: 2395-4396, Volume 5, Issue 2 2019	1	4.06
4	International	Mr. Praful Pathare, Mr. Gurjit Singh Saini	EXTC	Security System using VILOA JONES face detection algorithm	IJARIE, Paper ID 10089, e-ISSN: 2395-4396, Volume 5, Issue 2 2019	1	4.06
5	International	Ms. Payal Das, Mr. Aditya Ghag, Ms. Lalita Maurya	EXTC	Handspeak System using Artificial intelligence	IRJET, e-ISSN 2395-0056, p-ISSN 2395-0072, Volume 6, Issu 1/Jan 2019	1	6.171
6	International	Prof. M.T. Bhagawati	PROD	Identifying key success factors of sustainability in supply chain management for industry 4.0 using DEMATEL method	Springer Nature Singapore Pte Ltd. 2019	1	
Total						6	



*henn*  
Dr. M. J. Lengare  
Principal  
Konkan Gyanpeeth  
College of Engineering  
Karjat 410 201

# **Appendix-I**

# **Appendix-I**

ICMPC 2017

# Carbon to Carbon Nanotubes Synthesis Process: An Experimental and Numerical Study

V. J. Pillewan<sup>a\*</sup>, D. N. Raut<sup>a</sup>, K. N. Patil<sup>b</sup>, D. K. Shinde<sup>a</sup>

<sup>a</sup>Department of Production Engineering, Veermata Jijabai Technological Institute, Matunga, Mumbai 400019, India

<sup>b</sup>Department of Mechanical Engineering, K. J. Somaiya College of Engineering, Mumbai 400077, India

---

## Abstract

The present work uses Co catalyst with CaCO<sub>3</sub> substrate for CNTs synthesis. The Co catalyst prepared with 1%, 3%, and 5% weight percentage. The CNTs synthesis is carried out from 600 to 750°C. It is observed that for 1% catalyst loading, purified CNTs obtained at 750°C is 0.8887 grams. The similar trends obtained for 3% and 5% catalyst weight percentage. Scanning Electron Microscope (SEM) images show large bundles of CNTs with the average diameter of 29.31nm. The CNTs production models are developed. It is observed that models developed are closely related to the experimental results with the error band of 14.28%.

© 2017 Elsevier Ltd. All rights reserved.

Selection and/or Peer-review under responsibility of 7th International Conference of Materials Processing and Characterization.

*Keywords:* Carbon Nanotubes; Chemical Vapor Deposition; Co catalyst; CaCO<sub>3</sub> substrate; Scanning Electron Microscope

---

## 1. Introduction

The material poised with Carbon Nanotubes (CNTs) is the area of keen interest now a day. Significant research has done on using CNTs to reinforce polymer and ceramic matrices [1]. Only a few groups have investigated CNTs based matrix with steel [2]. Carbon nanotubes are found an increasing interest as reinforcement for Fe/Al matrix due to their excellent mechanical properties. Couateau et al. [3] proposed the large-scale synthesis of Multi –Wall Carbon Nanotubes (MWNTs) on CaCO<sub>3</sub> substrate with Fe-Co catalyst. The rotary CVD furnace is used for continuous production of high-quality MWNTs at a rate of 0.0694g/min. Choi et al. [4] proposed an economical synthesis

\* Corresponding author. Tel.: +91-9881273667

E-mail address: [v\\_pillewan@rediffmail.com](mailto:v_pillewan@rediffmail.com)

2214-7853© 2017 Elsevier Ltd. All rights reserved.

Selection and/or Peer-review under responsibility of 7th International Conference of Materials Processing and Characterization.

method for CNTs in large quantity using the dispersion of Nano-metal powders and magnetic fluid as catalysts. The metal catalyst is deposited on the plane substrates which has the limited area. Thus, this method is not useful for high yield CNTs synthesis. To overcome this restriction, spin coating of catalyst nanoparticles on Si particles is done. Li et al. [5] proposed the method of CNT formation with Ni/Mo as a catalyst and MgO as a substrate. The precursors used are methane-hydrogen in the nitrogen atmosphere. The process mainly produces high-quality MWNTs. The high purity of prepared MWNTs allows omitting the usual complex purification process required for CNTs synthesized by CVD method. High activity of Ni/Mo/MgO catalyst in its pristine state is ideal for mass production of high-quality MWNTs. The synergism of Ni and Mo is considered as the main reason for the high yield of CNTs. Willems et al. [6] used MgO as a substrate and Co, Co-Vanadium and Co-Fe as catalysts and acetylene as a precursor. Carbon Nanotubes produced with Co alone are much thinner and of more regular size distribution than the ones synthesized with metal mixtures. The amount of carbon deposit is higher for mixed metals than Co alone. The carbon deposit obtained with only Co catalyst is 20%. However, with Co-Fe catalyst amount of carbon deposit is as high as 75%. Louies et al. [7] used ethane as a precursor with Fe-Al<sub>2</sub>O<sub>3</sub> as a catalyst-substrate for the MWNT synthesis. It is reported that maximum yield obtained is 0.833 gCarbon/gFe/min at 750°C. Kabira et al. [8] have reported a rate of 0.378 gCarbon/gCo-Mo/min at 800°C with MgO substrate. The product contains 90% MWNTs after purification. The average diameter of the tubes obtained is 15 nm. Similarly, different substrates are studied in the literature for CNTs synthesis and the corresponding yields are listed in Table1 [9,10,11,12,13,14]. It shows that the CNTs yield strongly depends on the synthesis temperature. Above 750°C, a slowdown in the formation of CNTs observed due to partial deactivation of the catalyst. Up to 600°C, CNTs are observed with the small amount of amorphous carbon.

Table 1 Summary of different methods of MWNTs mass production by CVD method.

Ref.	Temperature	Substrate	Catalyst	Precursor	Yield
3	700-900°C	CaCO <sub>3</sub>	Ferric nitrate	C <sub>2</sub> H <sub>2</sub>	0.0694 g/min
5	650-1000°C	MgO	Ni/Mo	CH <sub>4</sub> /H <sub>2</sub>	0.033 gCNT/gNi-Mo/min
7	750°C	Al <sub>2</sub> O <sub>3</sub>	Fe	C <sub>2</sub> H <sub>6</sub>	0.833 gC/gFe/min
8	800°C	MgO	Co-Mo	C <sub>2</sub> H <sub>2</sub> /H <sub>2</sub>	0.378 gC/gCo-Mo/min
9	700°C	Carbon black powder	Co	C <sub>2</sub> H <sub>2</sub>	0.0636 gCNT/gCo/min
10	650°C	Al powder	Ni	CH <sub>4</sub>	0.2 gCNT/gNi/min
11	900°C	MgO	Fe-Ni-Mo	CH <sub>4</sub>	0.2216 gCNT/gCa/min
12	550°C	Al <sub>2</sub> O <sub>3</sub>	Co-Mo	CH <sub>4</sub>	0.03891 gC/gCa/min
13	800°C	Quartz Wafer	Ferrocene	Cyclohexane	0.0073 gCNT/g/min
		Al <sub>2</sub> O <sub>3</sub>	Fe-Mo		0.0106 gCNT/g/min
14	700°C	CaCO <sub>3</sub>	Fe	C <sub>2</sub> H <sub>2</sub>	1.21 gCNT/gCa/min
15	700°C	Quartz Tube	Ferrocene	Xylene	25% of feed stock
16	700°C	-	Ni	C <sub>2</sub> H <sub>2</sub>	0.216 gC/gCa/min
			Fe		0.483 gC/gCa/min
			Ni		0.700 gC/gCa/min
			Fe	C <sub>2</sub> H <sub>6</sub>	0.358 gC/gCa/min
			Fe-Ni		0.433 gC/gCa/min

Andrews et al. [15] discussed the CNTs synthesis process for the commercial application. They used two stage tubular furnace with ferrocene and xylene as a catalyst and precursor source, respectively. They claimed that 25% of the feedstock is converted into the MWNTs. Zeng et al. [16] demonstrated the formation of CNTs for two precursors such as acetylene and ethane. Three different catalysts used for synthesis are Fe, Ni, and Fe-Ni at a temperature of 700°C. They concluded that the yield variation occurred due to change in reactor dimension. Therefore, three different tubular reactors (44 mm, 70 mm and 120 mm) are used for synthesis.

Wei et al. [17] group from Tsinghua university, China demonstrated CNTs synthesis in a pilot plant to produce MWNTs at a rate of 25 g/min. They used fluidized bed furnace for deposition. The catalyst used for deposition is Fe-Mo and  $\text{Al}_2\text{O}_3$  as a substrate. The different precursors and catalyst used for CNTs synthesis reported in the literature. Chemical Vapor Deposition strongly depends on the experimental conditions which include the preparation and pre-treatment of the catalyst and the synthesis conditions [18]. The structural features of carbon nanotubes grown by various kinetic models for CNTs synthesis are reported in the literature but experimental validation is inadequate and needs further attention.

Carbon Nanotubes are required in large quantity and the reported yield of CNTs ranges only a few milligrams to grams per batch. Moreover, the conversion efficiencies are very poor thereby increasing the cost of CNTs. Hence, a systematic parametric optimization is required in view of high yield CNTs synthesis. This paper studies various steps of carbon to CNTs conversion namely, precursor decomposition at catalyst surface, CNTs yields during purification and annealing. Also, discusses kinetic models based on the experimental results to study the carbon decomposition process. The PLM and SOPM are developed to study the carbon to CNT synthesis. The methodology is developed to achieve maximum utilization of decomposed carbon for CNTs conversion. The carbon balance at every stage is observed. Carbon loss and its efficiency are evaluated at each stage.

## 2. CNT Catalysts and CNTs Synthesis

Generally, catalysts used for CNTs synthesis are transition metals. Fe, Co, and Ni are the most effective and widely used transition metals, because of two main reasons: (i) high solubility of carbon at high temperatures; and (ii) high carbon diffusion rate. Recent considerations are Fe, Co, and Ni have stronger adhesion with the growing CNTs (than other transition metals do) and hence they are more efficient in forming low diameter CNTs.

General experience is that low-temperature CVD (600–900°C) yields MWCNTs, whereas high-temperature reaction (900–1200°C) favors SWCNT growth. This indicates that SWCNTs have a higher energy of formation (most probably due to small diameters; high curvature bears high strain energy). By proper selection of CNT precursor, both the catalyst's lifetime and the CNT-growth rate can be significantly increased; and consequently, both the yield and the quality of CNTs can be improved. Also, the quality of CNTs highly depends on the method of purification. A three-stage purification method is used in this study so that the consistency in the quality of CNTs can be ensured.

The different substrates used for the CNTs formation are  $\text{CaCO}_3$ , MgO,  $\text{Al}_2\text{O}_3$ , and  $\text{SiO}_2$ . Magnesium Oxides substrate is widely used because it is easily dissolved in the purification process with HCL. But for purification, carbon deposit obtained with  $\text{SiO}_2$  substrate needs the hazardous chemicals and it is difficult to clean the CNTs. Hence  $\text{CaCO}_3$  is used as a substrate as it decomposes into CaO at 712°C and easily removed with the help of acids during the purification process.

## 3. Experimental procedure

Figure 1 shows a photograph of experimental set-up and its schematic diagram used for CNT growth by CVD method. The process involves passing an acetylene gas vapor (60 min.) through a horizontal tubular furnace in which a catalyst material is present at the sufficiently high temperature (600–1200°C) to decompose the hydrocarbon. CNTs growth on the catalyst depends on precursors flow rate, deposition time, and reactor geometry. Most commonly used CNT precursors are acetylene, methane, benzene, xylene and carbon monoxide. Cobalt Nitrate ( $\text{Co}(\text{NO}_3)_2 \cdot 6\text{H}_2\text{O}$ ) is used as catalyst precursors while  $\text{CaCO}_3$ , in fine powder form, is used as a substrate. The samples are prepared by mixing measured amount of catalyst precursors and substrate in deionized (DI) water. Thereafter, water is removed from the mixture by evaporating at 100°C followed by subsequent cooling in moisture proof atmosphere. The as-prepared catalyst is used for CNT deposition. The flow rates of precursor gas (acetylene) and carrier gas (argon) are maintained at 60 ml/min and 100 ml/min, respectively. The experiments are carried out over a temperature range of 600–750°C in steps of 50°C. For each temperature, the time of precursor flow is 30 min. After calculating theoretical carbon deposition and weighing experimental carbon deposition, CNT purification process by HCL and  $\text{HNO}_3$  are carried out.

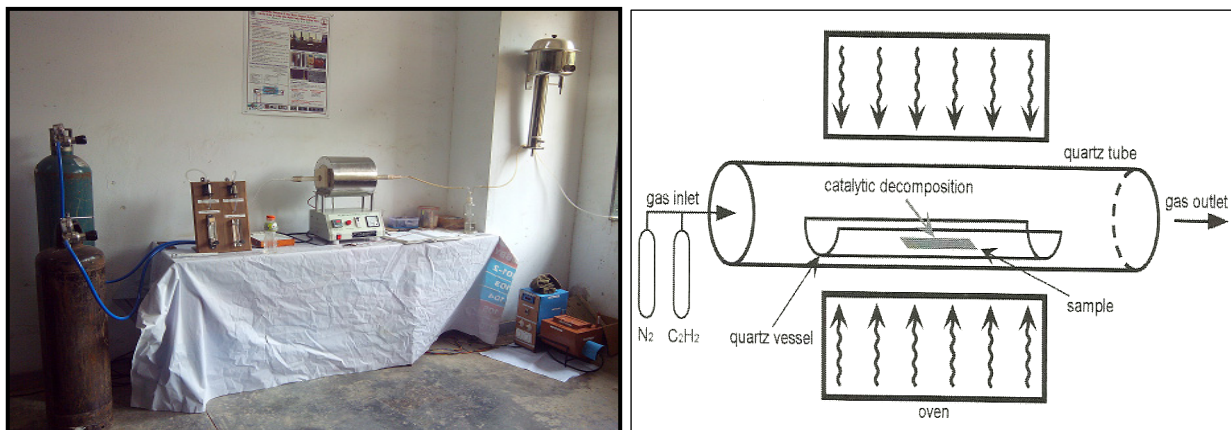


Fig. 1. Experimental diagram of a CVD setup (Actual and Schematic [19]).

Figure 2 (A) shows a mixture of catalyst and substrate placed in a quartz boat which helps for CNT propagation on its surface after precursor gas effect. Figure 2 (B) shows the conversion of catalyst-substrate into unpurified CNTs by controlling various parameters. The quality of CNTs highly depends on the method of purification. The CVD deposit is treated with a 49% concentrated HCL solution for 24 hours followed by treatment with HNO<sub>3</sub> for 24 hours. These acids are used to remove the metal catalysts, amorphous carbon and calcium oxide (CaO). Eventually, all the samples are rinsed with deionized water and dried at 120°C. Figure 3 (A) and (B) shows three-stage purification and filtration process uses to clean the CNTs so that the consistency in the quality of CNTs can be ensured.

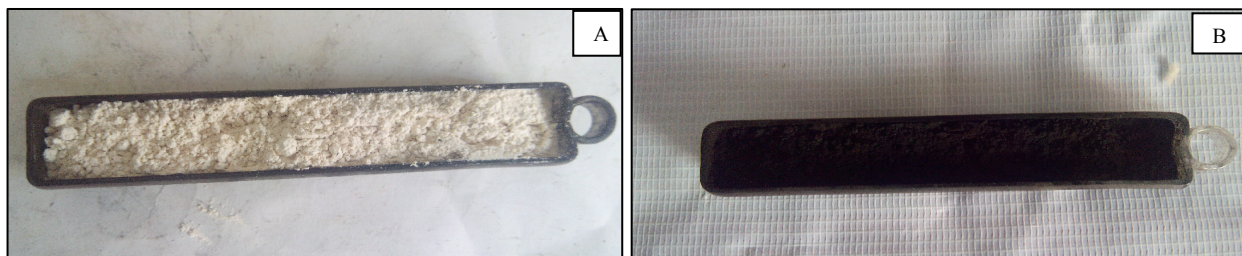


Fig. 2. (A) - Catalysts, (B) - Unpurified CNTs

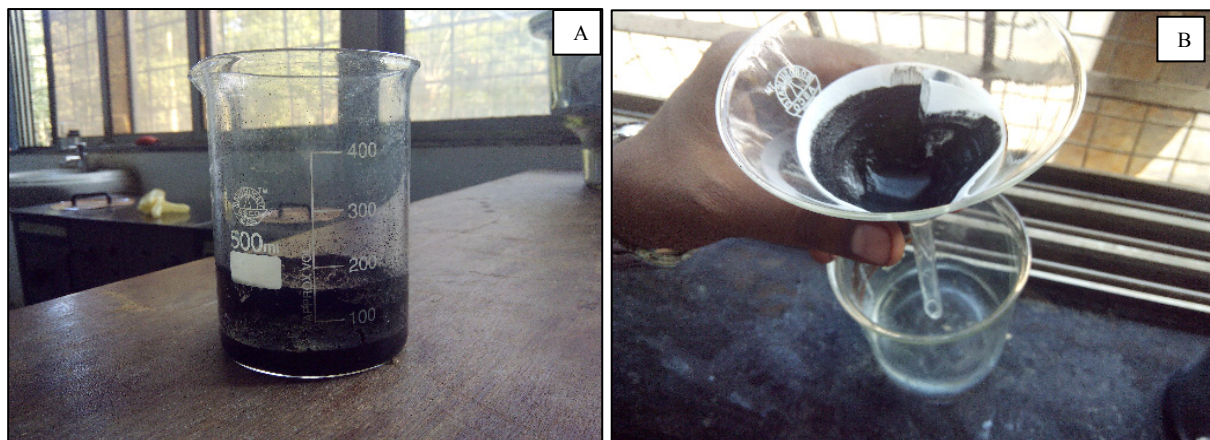


Fig. 3. (A) Acid treatments of CNTs and (B) Filtration of CNTs.



Figure 4 (A and B) shows SEM images of unpurified CNTs with the presence of some catalyst and substrate impurities. It is observed that the diameter of the unpurified CNTs varies in the range of 20 to 45 nm whereas the length is in few microns. Figure 4 (C and D) shows the purified CNTs. It is clearly observed that all catalyst and amorphous carbon impurities are removed during acid cleaning process. Table 2 observed that the diameter of the CNTs varies in the range of 15 to 40 nm. The average diameter of the purified CNTs is 29.31nm, evaluated by ImageJ software which is within the range of average nanoparticle size of Fe, Co, and Ni. Figure 4 (D) observed large bundles of CNTs reflecting uniform diameter and reasonable purity produced by CVD method.

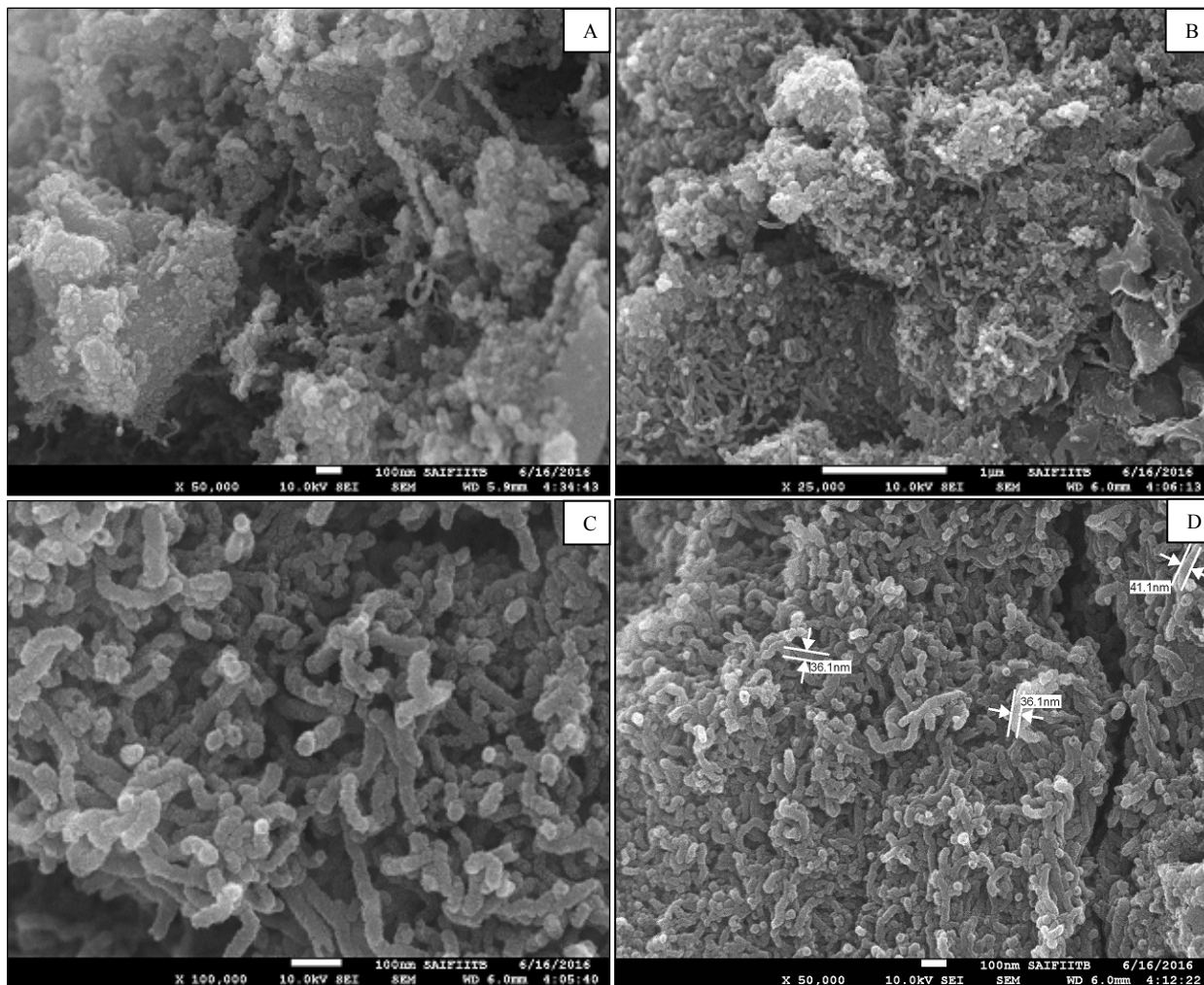


Fig. 4. SEM images of Unpurified CNT with Catalyst (A and B) and Purified CNT (C and D). (SAIF, IITB)

Table 2 Diameter of randomly selected Purified CNTs (Fig. 3 C)

CNT No.	1	2	3	4	5	6	7	8	9	10	11	12
Dia. (nm)	20.19	25.26	25.86	28.87	26.21	32.56	21.08	27.43	34.06	26.56	28.56	28.73
CNT No.	13	14	15	16	17	18	19	20	21	22	23	24
Dia. (nm)	37.80	28.05	25.42	29.81	16.28	32.59	29.71	39.49	38.42	31.41	32.09	36.71

#### 4. Results And Discussion

Table 3 shows the summary of the carbon to CNTs conversion efficiencies after each stage of CNTs synthesis process at various temperatures. The efficiency of CNTs formation for sample A at 750°C is 50.21%, whereas for sample B at 750°C, it is 39.07% at given catalyst loading. However, the carbon to CNTs conversion efficiency stabilizes at around 700°C. As the catalytic activity of the catalyst reduces after 700°C, the improvement in the carbon to CNTs conversion efficiency is insignificant. Though higher carbon deposition observed at 750°C due to more of amorphous carbon and thus effectively less CNT are produced. It is seen that carbon conversion efficiency increases with an increase in temperature up to 700°C.

A kinetic analysis is carried out to compare the model value and experimental value related to CNTs deposition. The general equations for the PLM and SOPM are shown respectively as follows:

$$M_c = aT^b \quad (1)$$

$$M_c = aT^2 + bT + c \quad (2)$$

Where,  $M_c$  is a Model value,  $T$  is a corresponding temperature and  $a$ ,  $b$  and  $c$  are constants.

The experimental CNTs deposit data fitted with PLM and SOPM. The second order polynomial fitted at lower temperature deviates significantly from the experimental CNTs deposit, however at higher temperature i.e. more than 650°C the error in the model value and the experimental data is less than 10%.

Table 4 and 5 shows the PLM and SOPM for sample B which predicted that model values much closer to the experimental data. Thus PLM is best suited as against to the SOPM.

Table 3 Carbon to CNT conversion Chart

Sample	Temp.	Experimental Carbon Deposition (gms)	Theoretical Carbon Deposition (gms)	Experimental Carbon Deposition (gms) with HCL	Experimental CNT (%) (gms) with HNO <sub>3</sub>	Experimental CNTs Deposition % after HCL	Experimental CNTs Deposition % after HNO <sub>3</sub>	Theoretical CNTs Deposition % after HCL	Theoretical CNTs Deposition % after HNO <sub>3</sub>
Sample A	600 <sup>o</sup> c	0.2398	0.3330	0.1937	0.1637	80.77	68.27	58.11	49.11
	650 <sup>o</sup> c	0.7003	0.9690	0.6476	0.5530	92.47	78.97	66.83	57.07
Cobalt (1%) + CaCO <sub>3</sub>	700 <sup>o</sup> c	1.1108	1.5810	1.0374	0.8288	93.40	74.62	65.62	52.42
	750 <sup>o</sup> c	1.2320	1.7700	1.1292	0.8887	91.66	72.13	63.79	50.21
Sample B	600 <sup>o</sup> c	0.2387	0.3330	0.1593	0.1432	66.74	59.99	47.79	42.96
	650 <sup>o</sup> c	0.6691	0.9690	0.6257	0.5817	93.52	86.94	64.57	60.03
	700 <sup>o</sup> c	0.9950	1.5810	0.7947	0.6499	79.87	65.32	50.27	41.11
Cobalt (5%) + CaCO <sub>3</sub> (95%)	750 <sup>o</sup> c	1.0983	1.7700	0.8402	0.6916	76.50	62.97	47.47	39.07

Table 4 Power Law Model for Sample B (Purified CNTs)

T	Mc	T* = logT	Mc* = logMc	T* x Mc*	T <sup>^2</sup>	Mc* = a*T <sup>^b</sup>	a	b	Error = Mc*- Mc
600	0.1432	2.778151	-0.84406	-2.34492	7.718124	0.206721	9.5959E-20	6.5991	0.06352054
650	0.5817	2.812913	-0.2353	-0.66188	7.912482	0.350576	9.5959E-20	6.5991	-0.231123949
700	0.6499	2.845098	-0.18715	-0.53247	8.094583	0.571705	9.5959E-20	6.5991	-0.078194738
750	0.6916	2.875061	-0.16015	-0.46043	8.265977	0.901369	9.5959E-20	6.5991	0.209768749
N=4		11.31122	-1.42666	-3.9997	31.99117				

Table 5 Second Order polynomial Model for Sample B (Purified CNTs)

T	Mc	T <sup>^2</sup>	T *Mc	T <sup>^3</sup>	T <sup>^4</sup>	T <sup>^2</sup> *Mc	Mc* = a* T <sup>^2</sup> +b* T +c	Error = Mc*- Mc
600	0.1432	360000	85.92	2.16E+08	1.3E+11	51552	0.295792	0.1526
650	0.5817	422500	378.105	2.75E+08	1.79E+11	245768.3	0.438866	-0.1428
700	0.6499	490000	454.93	3.43E+08	2.4E+11	318451	0.588083	-0.0618
750	0.6916	562500	518.7	4.22E+08	3.16E+11	389025	0.743444	0.0518
2700	2.0664	1835000	1437.655	1.26E+09	8.65E+11	1004796		
	a = -0.9419		b = 0.0013256		c = 1.2287E-06			

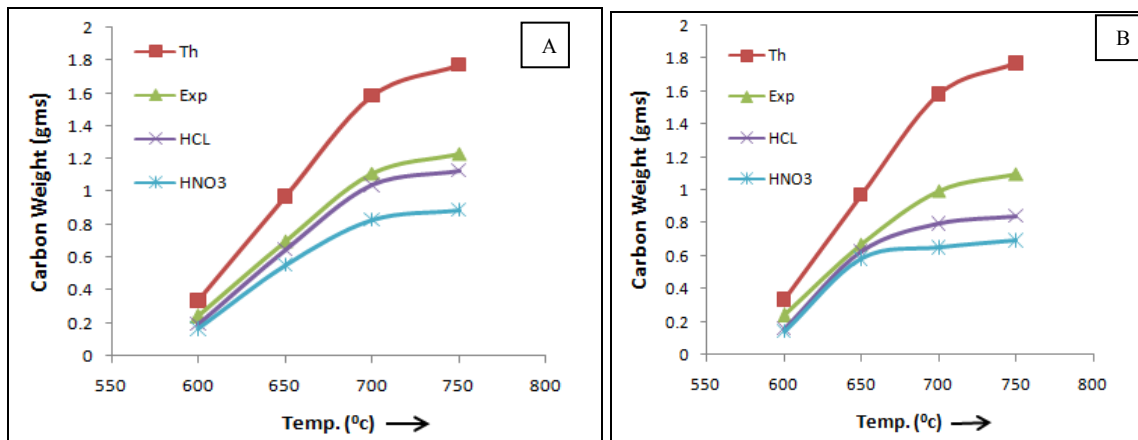


Figure 5 Carbon depositions Vs Temperature for sample A, and B

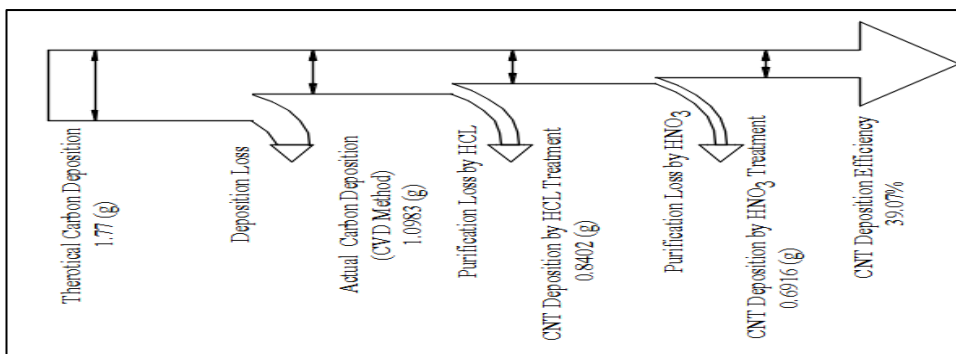


Figure 6 Sankey diagram representation of an amount of carbon available at each stage of CNTs deposition for sample B at temperature 750°C.

Figure 5 shows carbon depositions versus temperature for sample A, and B. For sample B, at temperature 750°C, it is observed that the amount of the carbon theoretically went to the reaction is 1.77 gm. However, the actual carbon deposit obtained is 1.0983 gm. After HNO<sub>3</sub> treatment the carbon deposit (CNTs purified) is 0.6916 gm with conversion efficiency 62.97%. Figure 6 shows the Sankey diagram of the carbon to CNTs formation. It is the scaled representation of the carbon content after each stage of CNTs synthesis (sample B) at 750°C with 60 ml/min acetylene flow rate. The actual carbon content after each stage is compared with the total carbon available for reaction. Then carbon conversion efficiency is calculated by taking the ratio of actual carbon content after each stage (obtained from measurement) to that of carbon available for the reaction (obtained from theoretical estimation).

## 5. Conclusions

It is observed that the amount of the carbon theoretically went to the reaction is 1.77 gm. However, the actual carbon deposit obtained is 1.0983 gm. After HCL treatment used for CNTs purification, the amount of carbon left is 0.8402 gm with the conversion efficiency of 76.50%. Further, after HNO<sub>3</sub> treatment the carbon deposit (CNTs purified) is 0.6916 gm with conversion efficiency is 62.97%. Sankey diagram represented for sample B at temperature 750°C, however, for all other active temperature zones, the carbon mass balances are carried out. Further, the mass balance is fitted with PLM and SOPM. It is observed that the both models closely correlate the process of CNTs synthesis. The highest theoretical efficiency for the carbon deposits is obtained as 60.03% at 650°C. Further, the maximum carbon to CNTs conversion is possible at 650°C with the conversion efficiency 86.94 % indicating that carbon conversion efficiency increases with an increase in temperature up to a certain limit (below 712°C). This may be due to losing the catalytic activity of the catalyst at high temperature as CaCO<sub>3</sub> decomposes into CaO at 712°C. Similarly, the average diameter of the purified CNTs is found to be 29.31nm, which is less than average nanoparticle size of Fe, Co, and Ni. Scanning Electron Microscopic images reflecting uniform diameter, reasonable purity and less defective CNT produced during CVD method.

## Acknowledgement

Authors acknowledge the financial support by A. T. E. Industries Pvt. Ltd. Mumbai for the given project.

- 
- [1] P.J.F. Harris., Carbon nanotube, *Int Mater Rev*, 2004.
  - [2] W.A.Curtin., B.W. Sheldon, CNT-reinforced ceramics, and metals, *Mater Today*, 2004.
  - [3] E. Couteau., K. Hernadi, J. W. Seo, L. Thien-Nga, Cs. Miko,R. Gaal and F. Farro, CVD synthesis of high-purity multiwalled CNTs using CaCO<sub>3</sub> catalyst support for large-scale production, *Chem. Phys. Lett.*, 2003.
  - [4] G.S. Choi., Y. S. Cho, K. H. Son and D. J. Kim, Mass production of CNTs using spin-coating of nanoparticles, *Microelectron Eng*, 2003.
  - [5] Y.Lai., X. B. Zhang, X. Y. Tao, J. M. Xu, W. Z. Huang, J. H. Luo, Z. Q. Luo, T. Li, F. Liu, Y. Bao and H. J. Geise, Mass production of high-quality multi-walled carbon nanotube bundles on a Ni/Mo/MgO catalyst, *Carbon*, 2005.
  - [6] I. Willems., Z. Konya, A. Fonseca and J. B. Nagy, Heterogeneous catalytic production and mechanical resistance of nanotubes prepared on magnesium oxide supported Co-based catalysts, *Appl. Catal. A: General*, 2002.
  - [7] B. Louis., G. Gulino, R. Vieira, J. Amadou, T. Dintzer, S. Galvagno, G. Centi, M. J. Ledoux and C. Pham-Huu, High yield synthesis of multi-walled carbon nanotubes by catalytic decomposition of ethane over iron supported on alumina catalyst, *Catal. Today*, (2005).
  - [8] A.K.M. FazleKibria., Md. Shajahan, Y. H. Mo, M. J. Kim and K. S. Nahm, Long activity of Co-Mo/MgO catalyst for the synthesis of carbon nanotubes in large-scale and application feasibility of the grown tubes, *Diamond Relat. Mater.*, 2004.
  - [9] K. Dasgupta., R. Venugopalan and D. Sathiyamoorthy, The production of high purity carbon nanotubes with high yield using cobalt formate catalyst on carbon black, *Mater. Lett.*, 2007.
  - [10] H. Li., Chunsheng Shi, Xiwen Du, Chunnian He, Jiajun L. and Naiqin Zhao, The influences of synthesis temperature and Ni catalyst on the growth of carbon nanotubes by chemical vapor deposition, *Mater. Lett.*, 2008.
  - [11] Y. Cui., Xiaofeng Wu, Hao Wu, YajunTian and Yunfa Chen, Optimization of synthesis condition for carbon nanotubes by chemical vapor deposition on Fe-Ni-Mo/MgO catalyst, *Mater. Lett.*, 2008.
  - [12] S.-P. Chai., Sharif Hussein Sharif Zein and Abdul Rahman Mohamed, The effect of reduction temperature on Co-Mo/Al<sub>2</sub>O<sub>3</sub> catalysts for carbon nanotubes formation, *Appl. Catal.*, 2007.

- [13] R. Xiang., GuohuaLuo, Zhou Yang, Qiang Zhang, WeizhongQian and Fei Wei, Large area growth of aligned CNT arrays on spheres: Cost performance and product control, *Mater. Lett.*, 2009.
- [14] K.N. Patil., and C. S. Solanki, Precursor to high purity carbon nanotubes: A step by step evaluation of carbon yield, *Journal of Nano Research*, 2009.
- [15] R. Andrews., D. Jacques, A.M. Rao, F. Derbyshire, D. Qian, X. Fan, E.C. Dickey and J. Chen, Continuous production of aligned carbon nanotubes: a step closer to commercial realization, *Chem. Phys.Lett.*, 1999.



ICMPC\_2018

# Wear Analysis of Charcoal, Unpurified Carbon Nanotubes and Purified Carbon Nanotubes based Metal Matrix Composite

V J Pillewan<sup>a</sup>, D N Raut<sup>a</sup>, K N Patil<sup>b</sup>

<sup>a</sup>Department of Production Engineering, Veermata Jijabai Technological Institute, Matunga, Mumbai 400019, India

<sup>b</sup>Department of Mechanical Engineering, K J Somaiya College of Engineering, Mumbai, 400077, India

---

## Abstract

The different materials used to improve the mechanical strengths such as carbon fibers, CNTs, and other alloy's. The present study focus on the iron based metal matrix composites with charcoal, unpurified and purified CNTs as a reinforcement with the varying percentage of each constituent from 1 to 5 weight %. The wear testing is carried out for five different pin loading varying from 1 to 5 kg. It is observed that as a percentage of the CNTs increase, the material shows more wear resistance characteristics. Experimental results confirmed that CNT based MMC is much tougher than the charcoal based MMC.

© 2018 Elsevier Ltd. All rights reserved.

Selection and/or Peer-review under responsibility of Materials Processing and characterization.

*Keywords:* Metal Matrix composite, Wear Testing, Carbon Nanotubes, Charcoal, Unpurified Carbon Nanotubes, Purified Carbon Nanotubes

---

## 1. Introduction

The different metals are used for the metal composite preparation such as Al, Ni, Fe, Mg, Ti, Ag and Cu etc. However, Fe/Al-based material is used for many applications as it is cheap, light in weight and good machinability. Different research groups are working on the Fe/Al metal matrix preparation with CNTs, providing high-quality material. The major concern in this process is the uniform dispersion of the carbon nanotubes in the Fe/Al powder mix. The different methods are used for uniform mixing.

\*Corresponding author:

Email Id: [v\\_pillewan@rediffmail.com](mailto:v_pillewan@rediffmail.com)

2214-7853 © 2018 Elsevier Ltd. All rights reserved.

Selection and/or Peer-review under responsibility of Materials Processing and characterization.

**Nomenclature**

Fe	Iron
MIM	Metal injection molding
MMC	Metal matrix composites
MWNT	Multiwalled carbon nanotubes
CNT	Carbon nanotubes

They reviewed critically about the carbon nanotubes-based metal matrix and suggested that a lot of emphases is given to the polymer and ceramic composites rather than metal matrix composites. These composites can be made by powder metallurgy route, melting and solidification, thermal spay, electrochemical deposition and other novel techniques etc. The powder metallurgy route is the most popular method for carbon nanotubes based metal composite preparation. This method is quite simple and involves lower temperature sintering which avoids damage to CNTs and gives better quality products. Some of the novel techniques are used for the metal composite preparation; however, these techniques are still in labs and large-scale implementation is a serious problem. Kuzumaki et al. [ v] concluded that CNTs withstand the extrusion force but they found in-homogeneity in the composite matrix. The higher percentage of the CNTs in the mix also creates agglomeration problem concluded by Deng et al. They suggest that 1 wt% CNTs gives better quality composite as compared to the 2 wt% CNTs mix. The interfacial bonding studies are carried out by different groups and it suggests that weak bonding cause's inferior mechanical properties. High strength and light weight material are mostly used in the aviation industry. Similarly, there are many applications where light weight with high strength materials is required in the automobile industry. However, to achieve this, either by providing high strength material or providing higher dimensions leads to increase in weight of the components. Thus, light weight carbon composite with the carbon nanotubes will be an ideal candidate for such light weight high strength applications.

Debinding process was accomplished on compacted articles at three different temperature ranges including 70, 80 and 90°C. Sintering process also was successfully accomplished on samples. For observing microstructures, the surface and cross-section of specimens were compared before and after debinding as well as after. Generally, this newly developed binder demonstrated a good potential for being utilized in MIM process .A powder with different combinations of binder systems and a binder system with different combinations of powder systems were investigated with a combined experimental and simulation study The injection moulding was performed with a developed binder system based on high-density polyethylene (HDPE), paraffin wax (PW) and stearic acid. A suitable formulation for powder injection moulding was chosen. The best results were found using solvent debinding followed by thermal debinding. Final parts had densities close to 99% after sintering at 1600°C during 2h

The determination of fracture toughness of the epoxy/MWCNT matrix was carried out by using a single edge notch bending (SENB) method according to the ASTM D5045-99. Four different weight percentage (wt %) of multi-walled carbon nanotubes (MWCNTs) contents were used, which were 0 wt.%, 0.1 wt.%, 0.55 wt.% and 1.0 wt.%. Epoxy binder and MWCNTs were mixed by using a mechanical stirrer for 10 minutes at 1500 rpm speed and was further sonicated for 30 minutes at 30 Hz amplitude in order to enhance the homogeneity of MWCNTs in the matrix. The mechanical and tribological behaviour of self-lubricating metallic nanocomposite reinforced by carbon us nano-materials such as CNT and graphene. It includes the development of self-lubricating nanocomposites, related issues in their processing, their characterization, and investigation of their tribological behaviour. The results reveal that adding CNT and graphene to metals decreases both coefficient of friction and wear rate as well as increases the tensile strength. The wear and frictional properties of metal matrix hybrid composites were studied by performing dry sliding wear test using a pin on disc wear test apparatus as per ASTM standards G-99. Experiments were conducted based on the plan of experiments generated through Taguchi's technique. An L9 Orthogonal array was selected for analysis of data. The wear behaviour of nano-composite with different CNT content were studied with a pin-on-disc tribometer, sliding against AISI52100 steel disc. Experiments were conducted using different sliding velocities of 0.5, 0.65 and 0.79 m/s and a normal load of 5.5, 7.2 and 10 N. From the wear map it is observed that

during dry sliding wear an increase of any of the operating condition such as normal applied load, sliding velocity, or duration of rubbing leads at some stage to a sudden change in the wear rate (weight loss per sliding distance). CNT-Al nano-composite shows lower wear rate than pure metal and wears rate of all the tested materials increases with increasing the normal applied load. Wear rate decreases with increasing CNT content from 0-1.5 wt% and increase slightly from 1.5-2 wt%, then increase rapidly after this range of CNT content .

## 2. Experimental Procedure

### 2.1 Debinding of samples

The grinding waste materials are added to the CNTs and binders. To form a green mixture, the grinding waste material, CNTs, binders are put in sigma mixer. The green mix is produced. Thereafter, test specimen is produced for various tests with the help of injection moulding machine along with suitable dies. The samples are to be restrained with wax and other binders. The removals of these binders are performed with the debinding operation followed by the sintering process. After cleaning the samples, different mechanical properties tests are performed with different analytical and spectroscopic tools. From Table 1, it is observed that Solvent debinding process removes complete wax added in the green sample. The few % of wax is trapped inside the green sample. It may be further removed during the sintering process.

Table 1 Estimation of solvent and thermal debinded of samples

Sample Type	Initial Mass (gms)	Target Mass	Solvent Debinding		Thermal debinding	
			Actual mass	% debinding	Actual mass	% debinding
B (87-13)	11.541	10.574	10.678	99.03	11.361	93.07
D (89-11)	11.026	10.254	10.794	94.99	11.009	93.14

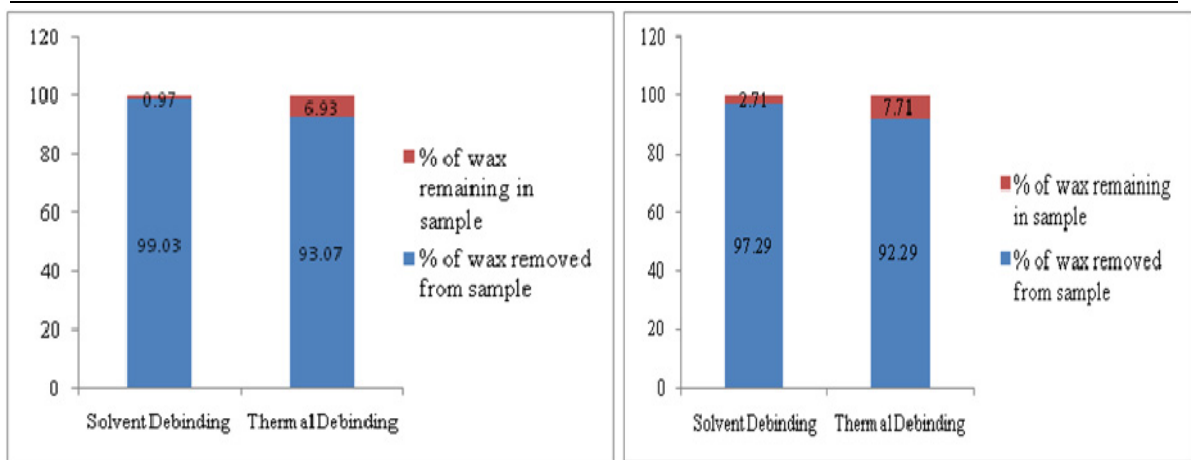


Figure 1 Wax removing process

### 2.2 Sintering of samples

The sintering is carried out between 800 to 1100°C in an inert ambient. The sintered samples were tested for wear testing as the application thought for the Fe-CNT MMC. The wear of sintered samples with varying load and varying % of Charcoal/UCNT/CNT were observed on Wear and Friction monitor (DUCOM-TR-20LE). The weight loss for the samples prepared was evaluated. The weight loss observed in between 0.49 to 10.63% after sintering of CNT samples, while the weight loss for the CNT sample is up to 2.08 after wear w.r.to sintering process. Table 2 shows the detailed weight loss analysis with various samples tested.



**3. Results and Discussion**

Figure 2 shows the actual setup for wear test with sintered samples. From the Table 2, it is observed that as the load on the sample A (1% CNTs) is increased from 1 kg to 5 kg wear on the composite material also increases. Similarly, the frictional force is also increased. After the certain time interval, the wear and frictional force get approximately constant. This shows that material gets more wear resistance after some time interval. Figure 3 shows the some wear samples with variable % of reinforcement which are sintered at 1100<sup>0</sup>

Table 2. Weight reduction of MMC-CNT samples during process

Load (Kg)	Sample (% CNT)	Wear (µm)	Friction Force (N)	Coeff. of Friction (µ)	% of Debinding (gm)	% of Reduction after Sintering	% of Reduction after Wear	Total % of Weight Reduction
1	A(1%)	153.6	2.27	0.231	97.11	0.49	2.86	7.02
	C(3%)	95.08	2.22	0.216	95.85	8.52	0.32	10.24
	E(5%)	11.12	1.44	0.156	98.33	5.98	1.21	10
3	A(1%)	386.6	16.63	0.553	97.05	0.97	0.61	5.26
	C(3%)	76.37	7.95	0.269	96.24	7.25	0.79	9.79
	E(5%)	3.39	2.84	0.101	95.79	10.63	1.16	12.12
5	A(1%)	464.0	11.53	0.226	93.94	7.90	0.85	9.21
	C(3%)	328.8	26.75	0.532	96.79	6.24	0.73	9.27
	E(5%)	184.3	10.16	0.201	98.28	4.86	1.09	8.76

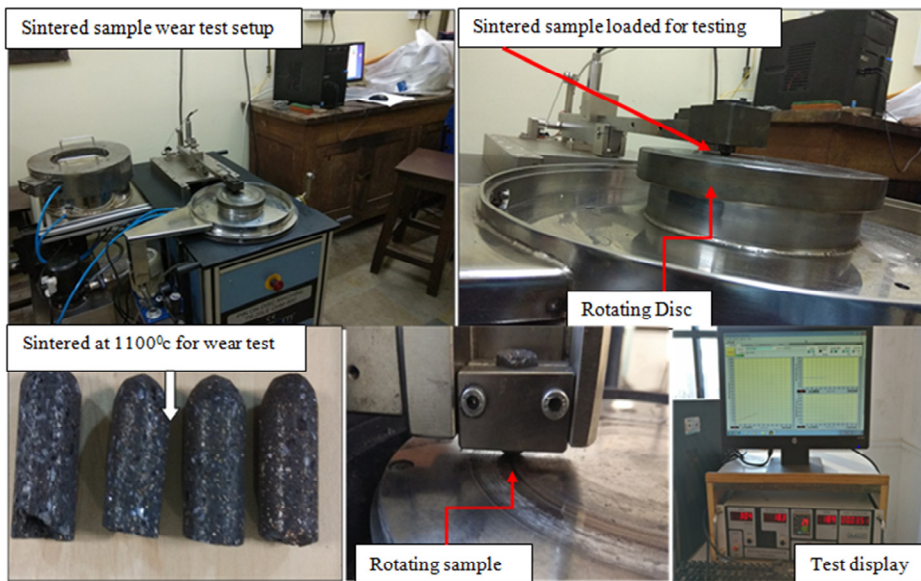


Figure 2 Experimental setup for wear test with variable % of Purified CNT sintered samples

Figure 2 Experimental setup for wear test with variable % of Purified CNT sintered samples

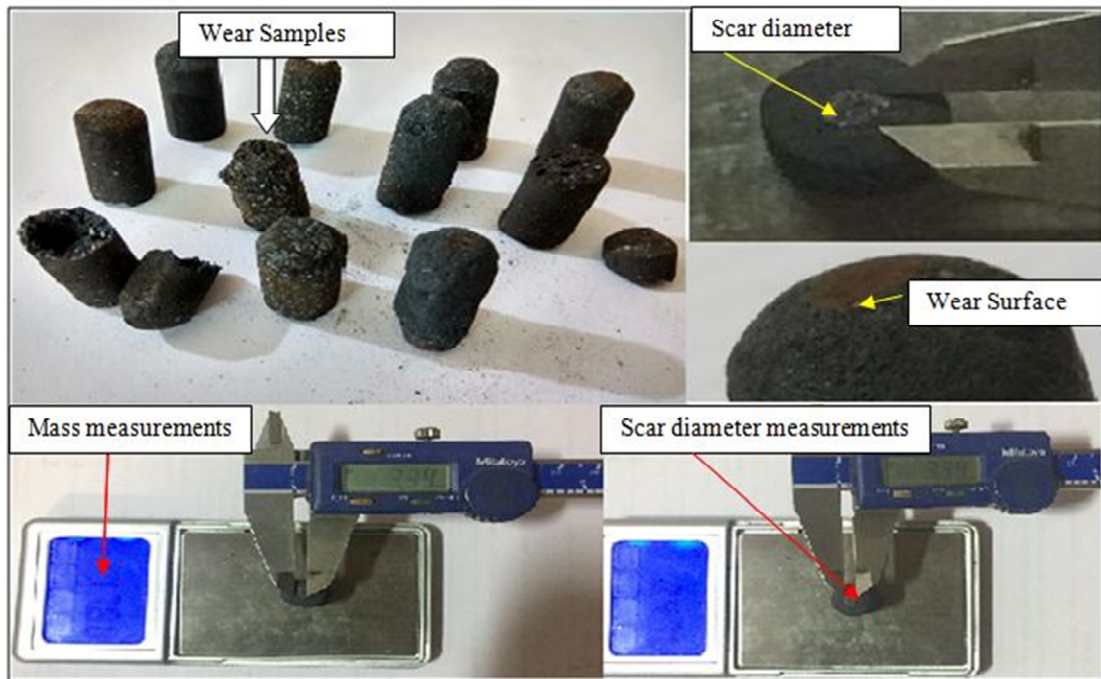


Figure 3 Wear test samples with variable % of reinforcement sintered at 1100°C

From the Table 2, it is observed that as the load on sample B is increased from 1 kg to 5 kg wear on the material also increases. Similarly, the frictional force is also increased. But sample B contained 2% percentage of CNTs, therefore, composite material wear resistance is more as compared to the sample A (1% CNTs). Also, frictional force resistance is increased. It is also observed that wear and frictional force graph is approximately horizontal after some time interval. It is observed that as the load on sample C is increased from 1 kg to 5 kg wear on the material also increases. Similarly, the frictional force is also increased. In case of sample C percentage of CNTs is 3%, therefore it has been seen sample C has more wear resistance than sample A and sample B. Also frictional force resistance is also increased. A wear and frictional force graph is approximately horizontal after 75 sec. and 30 sec. respectively. The same trend is observed for sample D and sample E. A wear and frictional force graph is approximately horizontal after 50 sec. and 30 sec. respectively. It is observed that as the load on the sample is increased from 1 kg to 5 kg wear on the material also increases. Similarly, the frictional force is also increased.

The Fe-CNTs metal matrix composite prepared with three different input carbon materials namely, charcoal, unpurified carbon nanotubes and purified carbon nanotubes. The novel method for the MMC sample preparation is used and explained elsewhere. The as-prepared MMC samples were sintered at 800°C to 1100°C. Sintered samples were tested with 1 kg load to 5 kg load for 300 seconds of time duration speed of the rotating disc is 200 rpm. The frictional forces carried by CNTs samples are always higher than charcoal and unpurified CNTs MMCs as evident from Figure 4 to Figure 8. The similar results were obtained for the wear for all MMCs prepared with the charcoal, unpurified and purified CNTs.

Figure 4 (a) shows the wear obtained with 1 % charcoal to the 5% charcoal added into the MMC sample. It is observed that the maximum wear obtained is around 40  $\mu\text{m}$  for 1% charcoal and as the percentage of the charcoal, additional increases to 5% the wear decrease drastically. Higher the percentage of the charcoal added the MMC become more brittle and it breaks when applied load on it. It is evident from the Figure 4 (a). Figure 4 (b) shows the frictional forces with the time for 1 kg load at various forces of charcoal i.e. 1 % to 5%. The maximum frictional

force the MMC samples carry is around 2.5 N with do not change significantly with increase in the percentage of the charcoal. Figure 4 (c) shows the wear obtained for unpurified CNTs and the wear increases to 60  $\mu\text{m}$  and to that for the purified CNTs is 150  $\mu\text{m}$  (Refer Figure 4 (e)). Thus it is evident that adding the more CNTs leads to tough and structures as against to the MMC prepared with charcoal samples. Figure 4 (d) and (f) shows the friction force obtained for the UCNTs and CNTs samples. It is observed that the frictional force resisted by the UCNTs samples is around 2.5 N while few MMC samples were broken study. The CNTs sample shows the frictional force resisted is in the ranges from 1.5 N to 2.5 N and all MMC show better resistance.

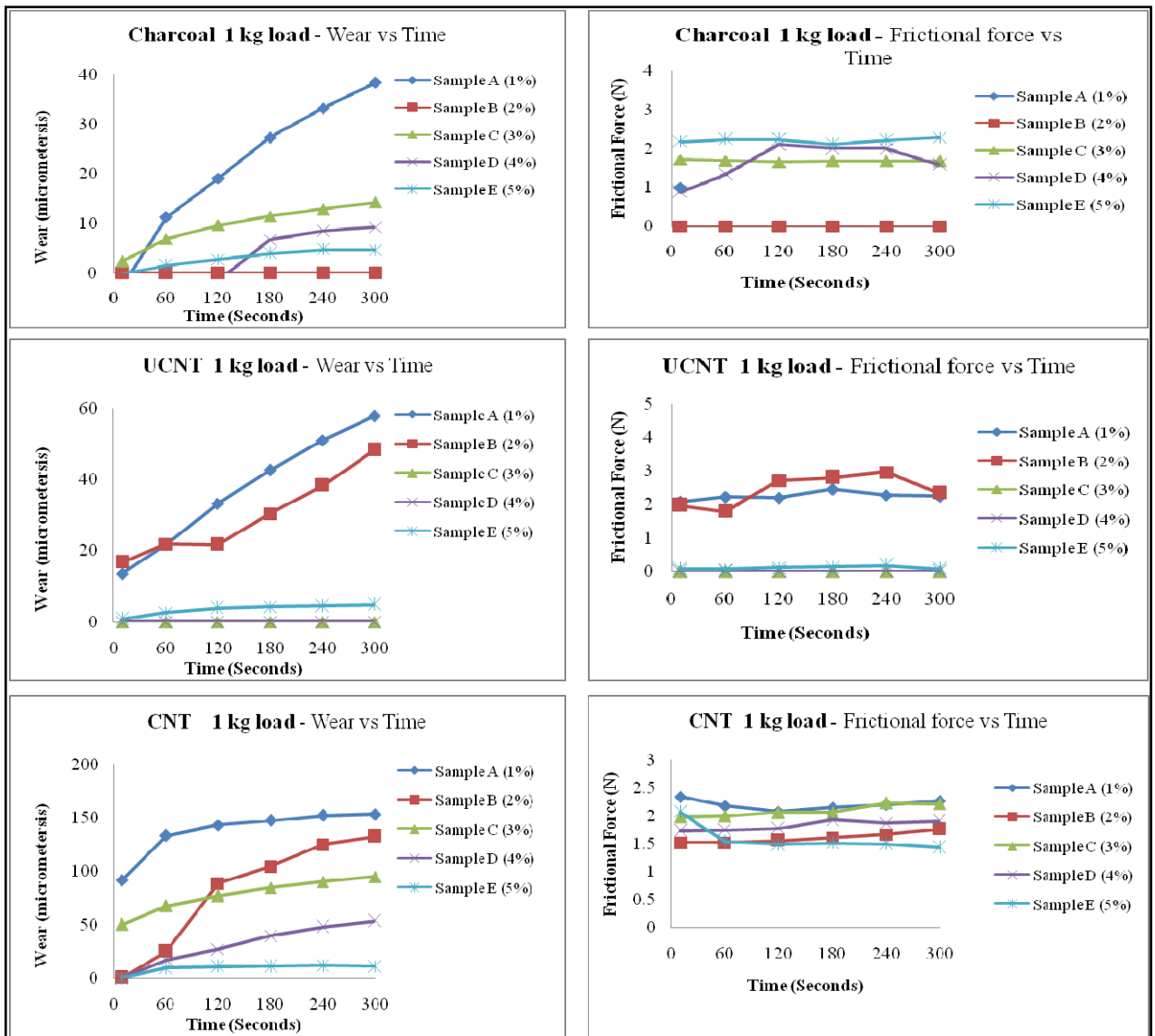


Figure 4 (a) Wear verses time for 1 kg load for 1% to 5% Charcoal composite, (b) frictional force verses time for 1 kg load for 1% to 5% Charcoal composite, (c) Wear verses time for 1 kg load for 1% to 5% UCNT composite, (d) frictional force verses time for 1 kg load for 1% to 5% UCNTs composite, (e) Wear verses time for 1 kg load for 1% to 5% CNT composite, (f) frictional force verses time for 1 kg load for 1% to 5% CNTs composite.

Similar study is carried out for the 2 Kg pin applied on the all three variety of sample prepared and it is obtained that the wear increase to double i.e. around 80 μm for 2 kg pin load (refer Figure 5 (a)) while the 180 μm for 3 kg load (refer Figure 6 (a)), 300μm for 4 kg load (refer Figure 7 (a)), 1100μm for 5 kg load (refer Figure 8 (a)) at for charcoal MMC samples. Thus it is observed that as load increase from 1 kg to 5 kg the wear increases with 25 times. Therefore at higher pin load the significant material removed from the MMC samples. Similar results are obtained for the frictional force and obtained at 2 kg load is 8 N (refer Figure 5 (d)), at 3 kg load, it is 14 N (refer Figure 7(b)), at 4 kg load, it is 16N (refer Figure 7 (b)) and at 5 kg load the frictional force is 22 N (refer Figure 8 (b)).

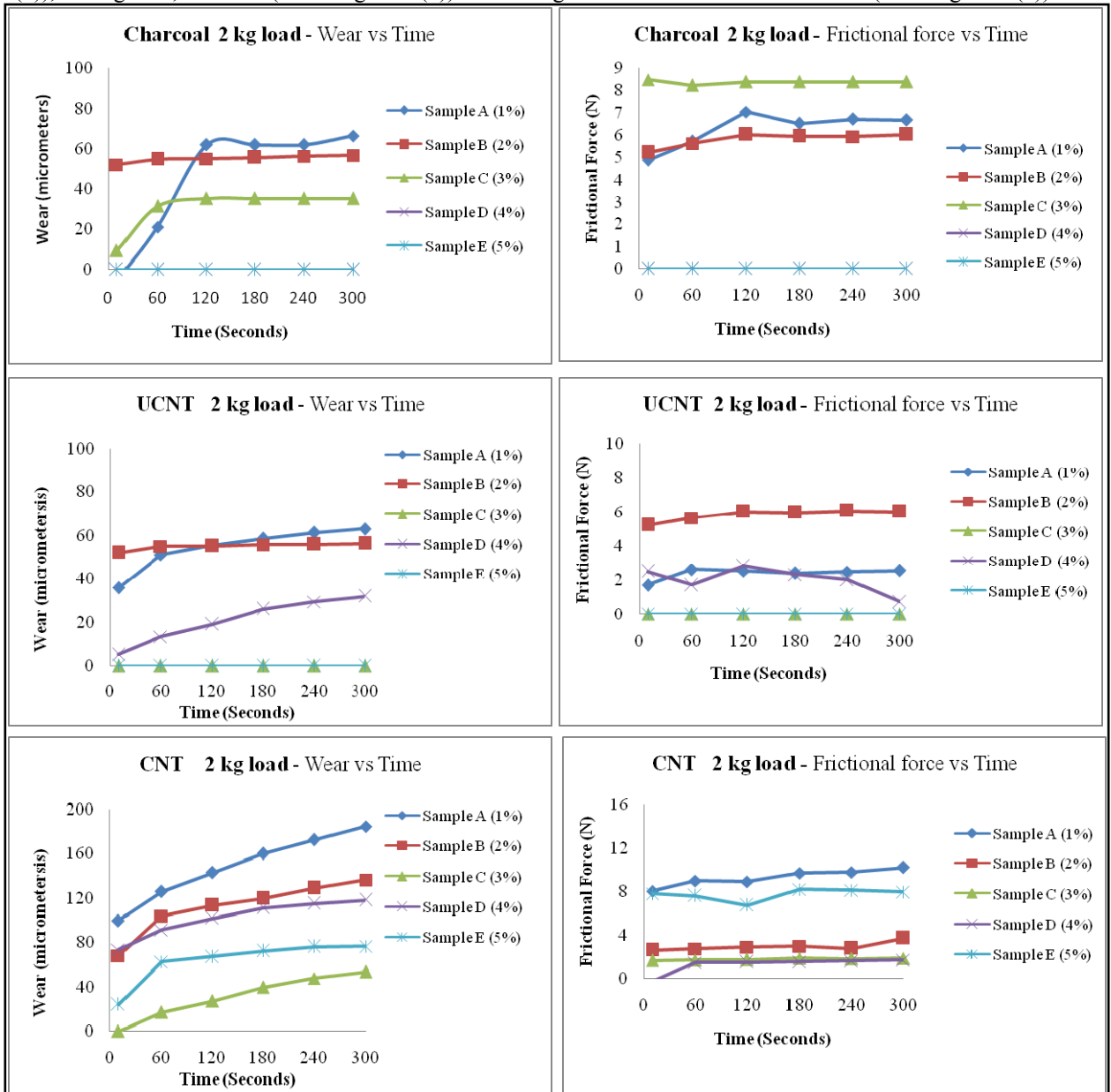


Figure 5 (a) Wear verses time for 2 kg load for 1% to 5% Charcoal composite, (b) frictional force verses time for 2 kg load for 1 % to 5% Charcoal composite, (c) Wear verses time for 2 kg load for 1% to 5% UCNT composite, (d) frictional force verses time for 2 kg load for 1 % to 5% UCNTs composite, (e) Wear verses time for 2 kg load for 1% to 5% CNT composite, (f) frictional force verses time for 2 kg load for 1 % to 5% CNTs composite.

The study is carried out for UCNT-MMC for 1 kg load to 5 kg pin load. It is observed that the wear increase from 60  $\mu\text{m}$  at 1 kg load to 900  $\mu\text{m}$  at 5 kg pin load. For 2 kg pin load (refer Figure 5 (c)) the wear is 70  $\mu\text{m}$ , for 3 kg load wear is 80  $\mu\text{m}$  (refer Figure 6 (c)), 350 $\mu\text{m}$  for 4 kg load (refer Figure 7(c)), 900  $\mu\text{m}$  for 5 kg load (refer Figure 8 (c)) at for UCNT-MMC samples. Thus it is observed that as load increase from 1 kg to 5 kg the wear increases with 13 times. Therefore, at higher pin load the material removal rate increases for UNCT-MMC samples but much less than the charcoal-MMC sample.

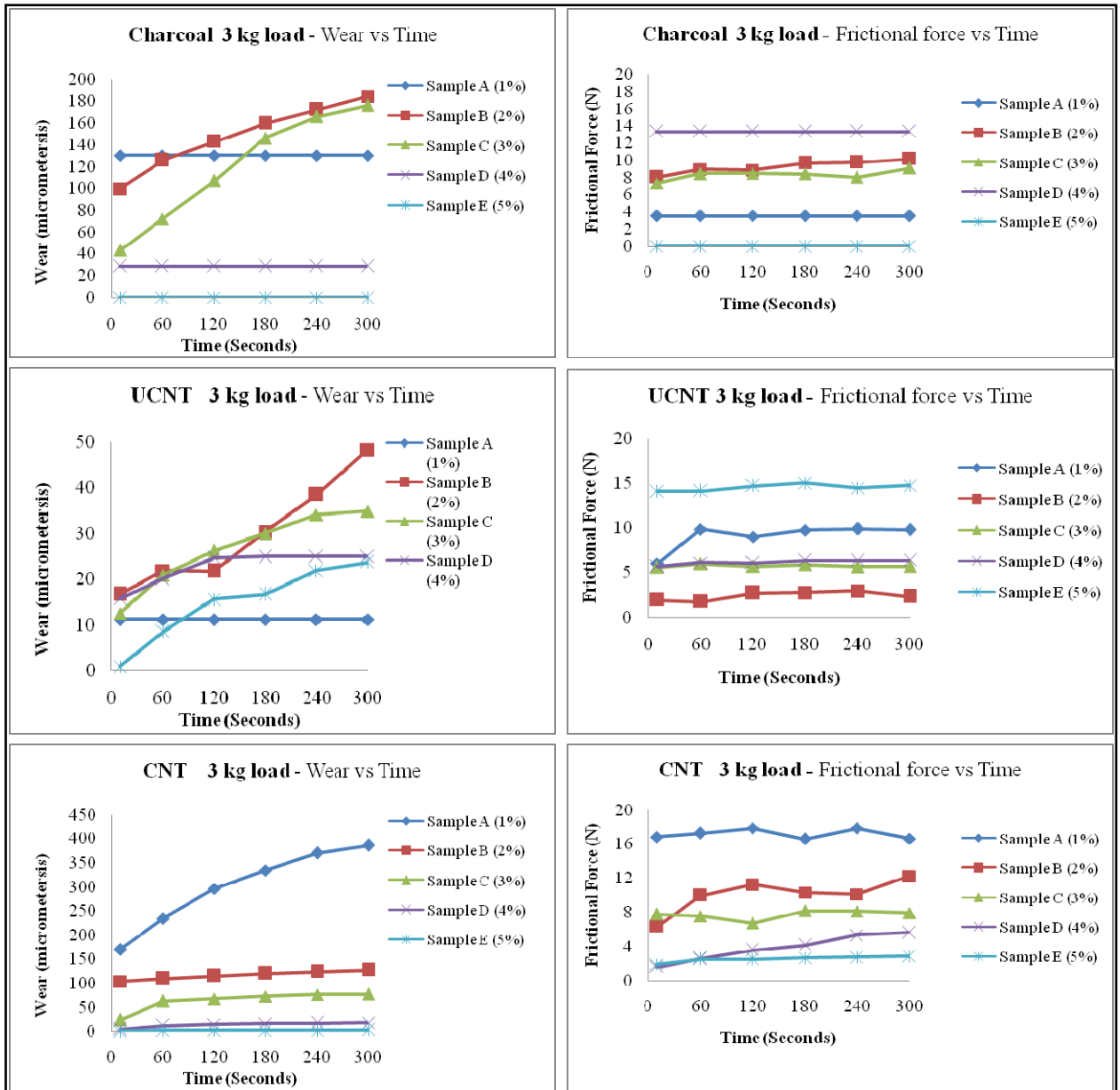


Figure 6 (a) Wear verses time for 3 kg load for 1% to 5% Charcoal composite, (b) frictional force verses time for 3 kg load for 1% to 5% Charcoal composite, (c) Wear verses time for 3 kg load for 1% to 5% UCNT composite, (d) frictional force verses time for 3 kg load for 1% to 5% UCNTs composite, (e) Wear verses time for 3 kg load for 1% to 5% CNT composite, (f) frictional force verses time for 3 kg load for 1% to 5% CNTs composite.

Similar results are obtained for the for frictional force the frictional force obtained at 2 kg load is 6 N (refer Figure 5 (d)), at 3 kg load frictional force is 12 N (refer Figure 7 (d)), at 4 kg load the frictional force is 15N (refer Figure 4 (d)) and at 5 kg load the frictional force is 25 N (refer Figure 8 (d)). The study is carried out for CNT-MMC for 1 kg load to 5 kg pin load. It is observed that the wear increase from 150 μm at 1 kg load to 400 μm at 5 kg pin load. For 2 kg pin load (refer Figure 5 (e)) the wear is 70 μm, for 3 kg load wear is 180 μm (refer Figure 6 (e)), 400 μm for 4 kg load (refer Figure 7 (e)), 400 μm for 5 kg load (refer Figure 8 (e)) at for UCNT-MMC samples.

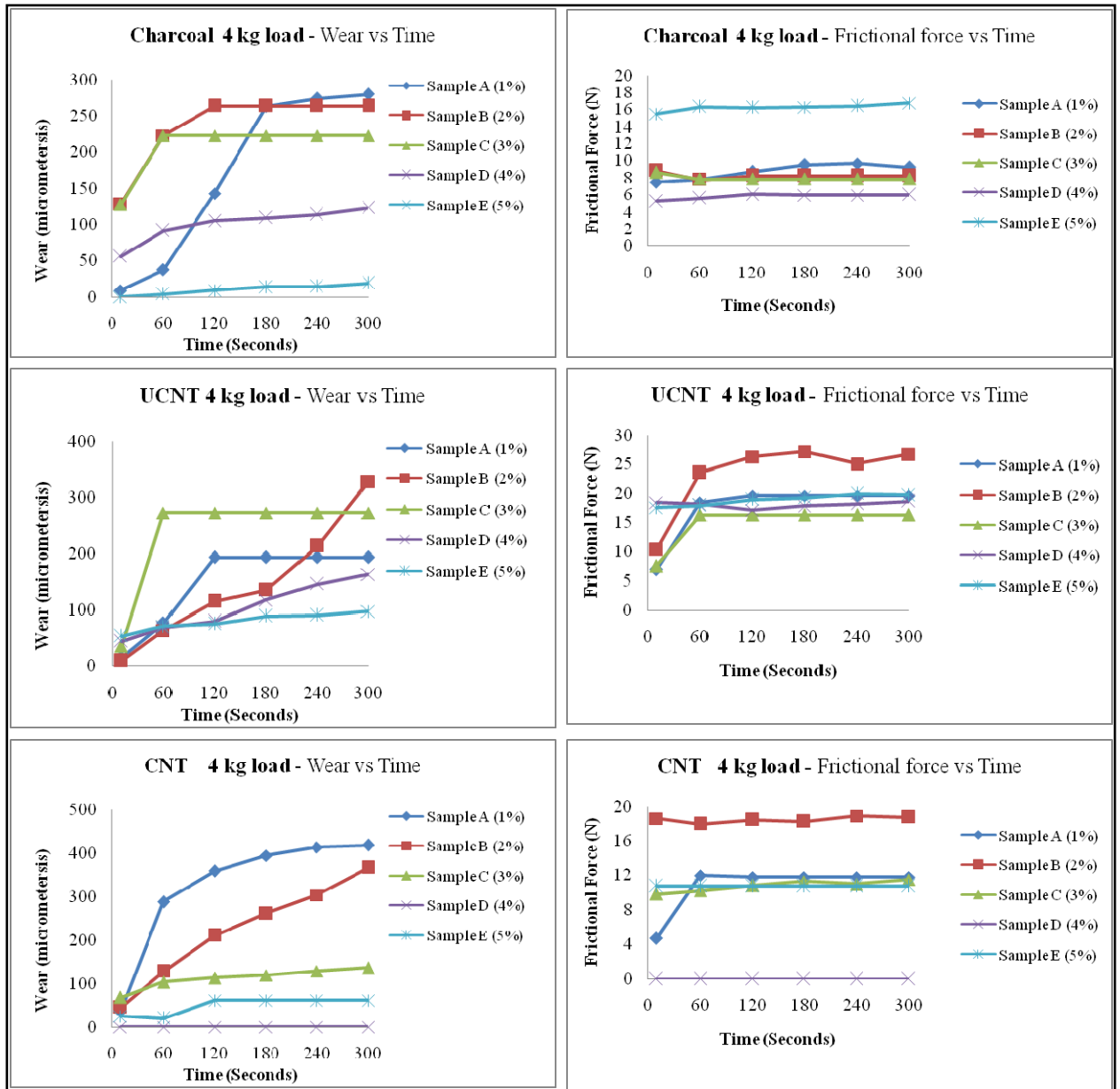


Figure 7 (a) Wear verses time for 4 kg load for 1% to 5% Charcoal composite, (b) frictional force verses time for 4 kg load for 1 % to 5% Charcoal composite, (c) Wear verses time for 4 kg load for 1% to 5% UCNT composite, (d) frictional force verses time for 4 kg load for 1 % to 5% UCNTs composite, (e) Wear verses time for 4 kg load for 1% to 5% CNT composite, (f) frictional force verses time for 4 kg load for 1 % to 5% CNTs composite.

Thus it is observed that as load increase from 1 kg to 5 kg the wear increases slightly. Therefore, at higher pin load the material removal rate increases for CNT-MMC samples but much less than the charcoal-MMC and UNCT-MMC sample. Similar results are obtained for the for frictional force the frictional force obtained at 2 kg load is 8 N (refer Figure 5 (f)), at 3 kg load frictional force is 16 N (refer Figure 7 (f)), at 4 kg load the frictional force is 20 N (refer Figure 7(f)) and at 5 kg load the frictional force is 25 N (refer Figure 8 (f)).

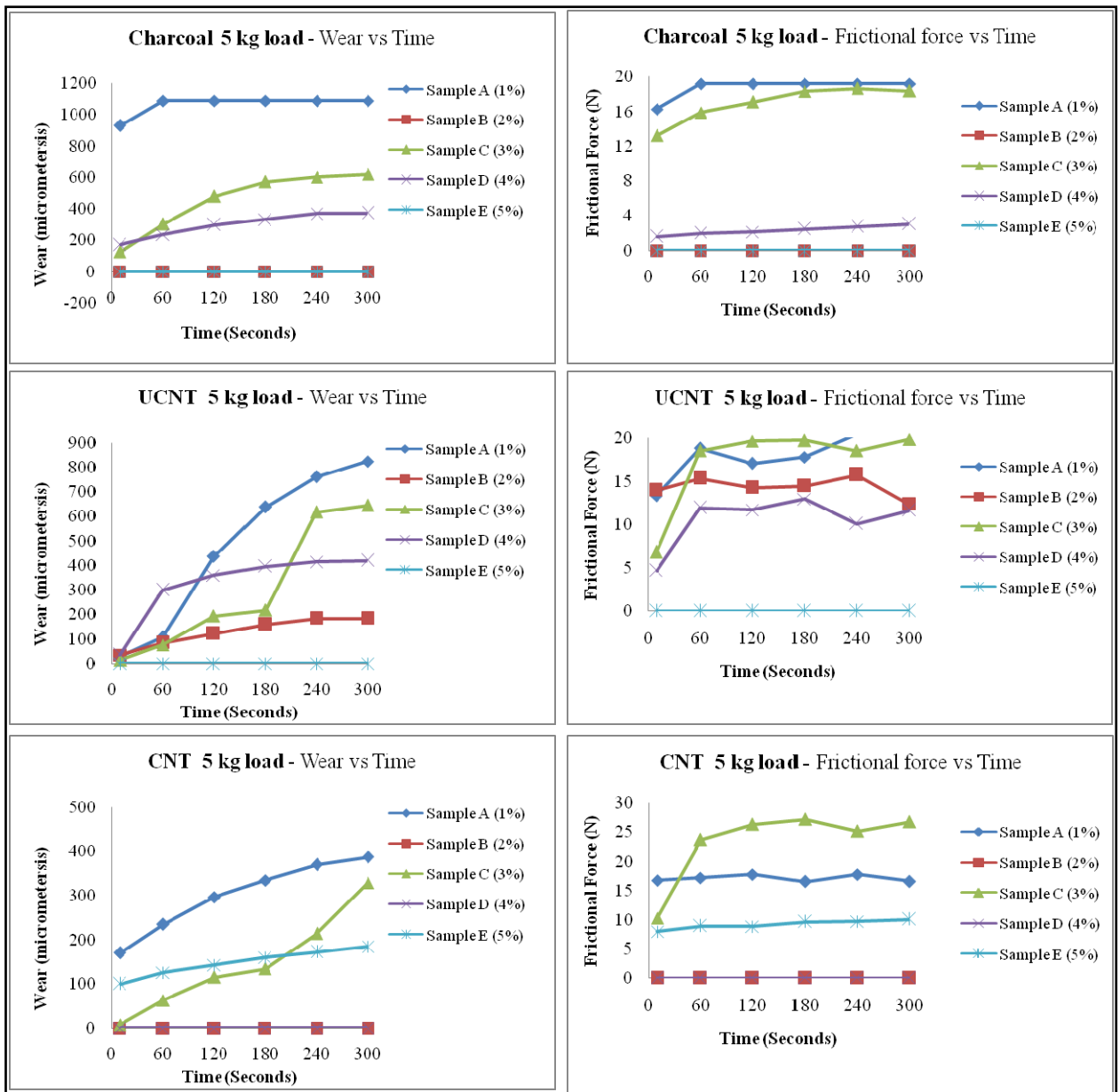


Figure 8 (a) Wear verses time for 5 kg load for 1% to 5% Charcoal composite, (b) frictional force verses time for 5 kg load for 1 % to 5% Charcoal composite, (c) Wear verses time for 5 kg load for 1% to 5% UCNT composite, (d) frictional force verses time for 5 kg load for 1 % to 5% UCNTs composite, (e) Wear verses time for 5 kg load for 1% to 5% CNT composite, (f) frictional force verses time for 5 kg load for 1 % to 5% CNTs composite.

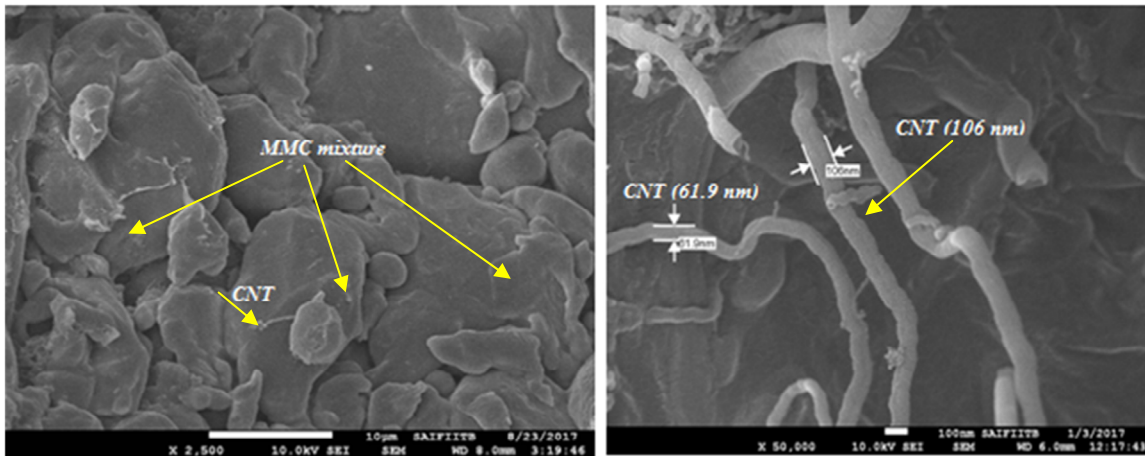


Figure 9 SEM images of iron composite with CNT dispersion

Figure 9, It is observed that the size of the purified CNTs varies from 61.1 nm to 106 nm. CNTs are well dispersed in the metal matrix composites. Some CNTs observed in the MMC mixture which improves the strength as well as wear and frictional resistance. The matrix structure is agglomeration free.

#### 4. Conclusions

The MMC samples were successfully fabricated with the various percentage of the carbon material. The different shape objects are prepared. It is observed that the samples are porous in nature. The different loads are used for wear testing. It is observed that the minimum wear obtained with the charcoal samples which are around 40  $\mu\text{m}$  at least loading while the maximum wear with the 900  $\mu\text{m}$  for UCNT samples and CNT-MMC samples shows 400  $\mu\text{m}$  wear. Further, it is observed the maximum frictional force carried by MMC samples is around 25 N for both samples with CNTs-MMC and UCNT-MMC samples. The CNTs-MMC and UCNTs-MMC show the better mechanical property as compared to the charcoal-MMC samples.

#### Reference

- [1] S. R. Bakshi, D. Lahiri and A. Agarwal, Carbon nanotube reinforced metal matrix composites- a review. *International Materials Reviews. Int. Mater. Rev.*, 55, 41-65,2010.
- [2] T. Noguchi, A. Magario, S. Fukazawa, S. Shimizu, J. Beppu and M. Seki, Carbon nanotube/ aluminium composites with uniform dispersion *Mater. Trans.*,45(2), 602-604,2004.
- [3] T. Laha, A. Agarwal, T. McKechnie and S. Seal, Synthesis and characterization of plasma spray formed a carbon nanotube reinforced aluminium composite, *Mater. Sci. Eng. A*, A381, 249-258,2004.
- [4] S. R. Bakshi, V. Singh, S. Seal and A. Agarwal, Aluminum composite reinforced with multiwalled carbon nanotubes from plasma spraying of spray dried powders, *Surf. Coat. Technol.*,203, 1544-1554,2009.



**Call for Papers:Vol.6 Issue.2**

**Important Dates**

Submission Last date	30-Apr-2020
Acceptance Status	In One Day
Paper Publish	In Two Days
<a href="#">Submit Manuscript</a>	

**News & Updates**

[News for bloggers](#)



Authors



Abstract



Citations



Downloads



Similar-Paper

**Authors**

*Title: : car locking and tracking*

*PaperId: : 10034*

*Published in: International Journal Of Advance Research And Innovative Ideas In Education*

*Publisher: IJARIE*

*e-ISSN: 2395-4396*

*Volume/Issue: Volume 5 Issue 2 2019*

*DUI: 16.0415/IJARIE-10034*

*Licence: : IJARIE is licensed under a Creative Commons Attribution-ShareAlike 4.0 International License.*

Author Name	Author Institute
Hitesh Bhoir	Konkan Gyanpeeth Collage of Engineering
Rakesh Pawar	Konkan Gyanpeeth Collage of Engineering,karjat
R.S.Meshram	Konkan Gvanpeeth Collage of Engineering,kariat

### Call for Papers:Vol.6 Issue.2

**Important Dates**

Submission Last date	30-Apr-2020
Acceptance Status	In One Day
Paper Publish	In Two Days

[Submit Manuscript](#)

### News & Updates

**News for bloggers**  
 వ్రాసేట వార్తలకు ఈ జర్నల్లో ప్రచురించుకోవాలంటే  
 on below link: [Join As Board](#)

[Authors](#)
[Abstract](#)
[Citations](#)
[Downloads](#)
[Similar-Paper](#)

### Authors

**Title :** SECURITY SYSTEM USING VIOLA JONES FACE DETECTION ALGORITHM  
**PaperId :** 10089  
**Published in:** International Journal Of Advance Research And Innovative Ideas In Education  
**Publisher:** IJARIE  
**e-ISSN:** 2395-4396  
**Volume/Issue:** Volume 5 Issue 2 2019  
**DUI:** 16.0415/IJARIE-10089  
**Licence :** IJARIE is licensed under a Creative Commons Attribution-ShareAlike 4.0 International License.

Author Name	Author Institute
Praful pathare	Konkan Gyanpeeth Collage of Engineering
gurjit singh saini	Konkan Gyanpeeth Collage of Engineering

# HANDSPEAK SYSTEM USING ARTIFICIAL INTELLIGENCE

Payal Das<sup>1</sup>, Aaditya Ghag<sup>2</sup>, Lalita Maurya<sup>3</sup>

<sup>1,2,3</sup>U.G. Student (BE), Department of Electronics and Telecommunication Engineering, Konkan Gyanpeeth College of Engg. Karjat, Maharashtra, India

\*\*\*

**Abstract** - A man-machine interaction project is described which aims to establish an automated voice to sign language translator for communication with the deaf using integrated open technologies. The first prototype consists of a robotic hand designed with low cost self designed Acrylic assembly which smoothly reproduces the alphabet of the sign language controlled by voice only. The core automation comprises an Arduino UNO controller used to activate a set of servo motors that follow instructions from a Raspberry Pi mini-computer having installed the open source speech recognition engine Julius. We discuss its features, limitations and possible future developments.

**Key Words:** Artificial Intelligence, Man-machine interaction, Open technologies.

## 1. INTRODUCTION

Sign language is a visual language that is used by deaf and dumb people as their mother tongue. Unlike acoustically conveyed sound patterns, sign language uses body language and manual communication to fluidly convey the thoughts of a person. It is achieved by simultaneously combining hand shapes, orientation and movement of the hands, arms or body, and facial expressions. It can be used by a person who has difficulties in speaking or by a person who can hear but could not speak and by normal people to communicate with hearing disabled people. As far as a deaf person is concerned, having access to a sign language is very important for their social, emotional and linguistic growth. Sign language should be recognized as the first language of deaf people and their education can be proceeded bilingually in the national sign language as well as national written or spoken language. Indian Sign Language is used by deaf, dumb and hard of hearing people for communication by showing signs using different parts of body. All around the world there are different communities of deaf and dumb people and thus the language of these communities will be different.

The Sign Language used in USA is American Sign Language (ASL); British Sign Language (BSL) is used in Britain; and Indian Sign Language (ISL) is used in India for expressing thoughts and communicating with each other. The "Indian Sign Language (ISL)" uses manual communication and body language (non-manual communication) to convey thoughts, ideas or feelings.

As we know it is not easy for a normal person to learn a Sign language to communicate with the deaf people therefore there is a need of automated system that will convert human speech into Standard Sign Language.

Our Voice to SL Translator consists of a robotic hand aiming to satisfy an important fundamental human need such as face to face communication.

In this way translation of the human voice into actual signs using a mechanical hand assembly with an electronic board able to command its fingers by voice inputs.

### 1.1 Standard Sign Language Chart



Fig 1 : Sign language for Alphabets



Fig 2 : Sign language for numeric

## 1.2 Block Diagram

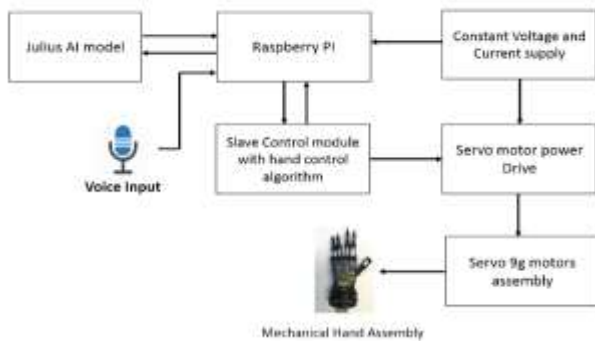


Fig. 2 : Block Diagram of HandSpeak System

This system comprises of a Robotic Hand which will show the sign language gestures corresponding to the user voice input. The user have to simply speak through the USB mic. Speech Recognition will be done by the Julius AI model which is running on the Raspberry Pi Operating System. Further Raspberry Pi will send the speech input in a proper serial format to the Arduino UNO which in turn will control the Robotic Arm.

## 2. Related Work

2.1. Mohamed Jemni, Oussama El Ghouli, Nour Ben Yahia, Mehrez Boulares.

### “SIGN LANGUAGE MMS TO MAKE CELL PHONES ACCESSIBLE TO DEAF AND HARD-OF-HEARING COMMUNITY”

Author proposed a system is developed to enhance communication with deaf, hard-of-hearing and speech disabled individuals. The originality of this tool consists on the use of new technologies to make the mobile phone a device of communication with deaf people and a tool for the integration of deaf to the society. They have tested this system by the Bluetooth, and they plan to test it really with an operator of telecom and to make it available as a new service of mobile phone.

## 3. Hardware Section

### 3.1 Raspberry Pi



Fig 3 : Raspberry Pi

The Raspberry Pi is a low-cost credit-card sized single-board computer. The Raspberry Pi was created in the UK by the Raspberry Pi Foundation. The Raspberry Pi Foundation's goal is to "advance the education of adults and children, particularly in the field of computers, computer science and related subjects. Many people have used the Raspberry Pi to make things like cameras, gaming machines, robots, web servers and media centres. There are a few different versions of the Raspberry Pi, each made for different uses. All of the current versions use a microSD card for the operating system and file storage. They are powered by a micro-USB port, have one HDMI port, one audio/video jack socket, and a 40-pin GPIO connector.

### 3.2 Arduino UNO



Fig 4 : Arduino Uno Board

Arduino is an open source computer hardware and software company, that designs and manufactures single-board microcontrollers and microcontroller kits for building digital devices and interactive objects that can sense and control objects in the physical world. Arduino board designs use a variety of microprocessors and controllers.

The boards are equipped with sets of digital and analog input/output (I/O) pins that may be interfaced to various expansion boards (*shields*) and other circuits. The boards feature serial communications interfaces, including Universal Serial Bus (USB) on some models, which are also used for loading programs from personal computers. The microcontrollers are typically programmed using a dialect of features from the programming languages C and C++. In addition to using traditional compiler toolchains, the Arduino project provides an integrated development environment (IDE) based on the Processing language project.

### 3.3 Mechanical Arm using servos

A mechanical arm is a machine that mimics the action of a human arm. Mechanical arms are composed of multiple beams connects by hinges powered by actuators. One end of the arm is attached to a firm base while the other has a tool. They can be controlled by humans either directly or over a distance. A computer-controlled mechanical arm is called a robotic arm. However, a robotic

arm is just one of many types of different mechanical arms.

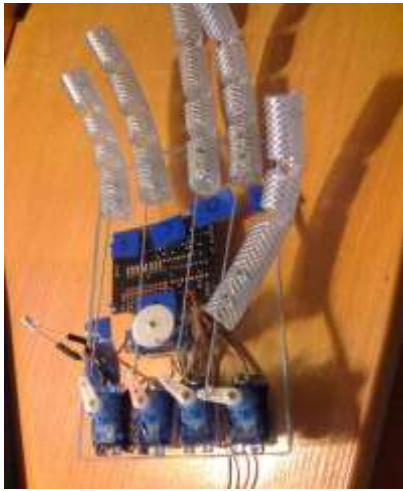
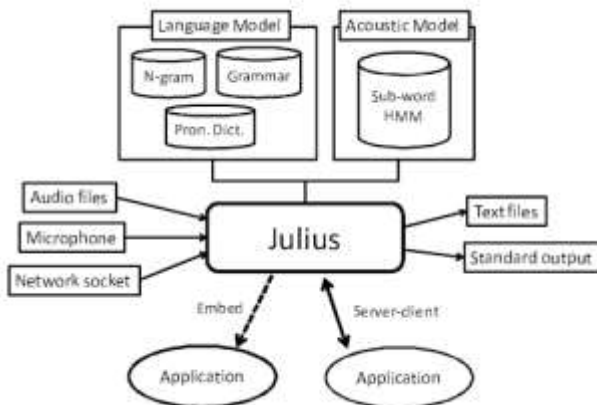


Fig 5: Mechanical arm using servos

#### 4. Software Section

##### 4.1 Julius AI model



Julius is an open-source large-vocabulary speech recognition software used for both academic research and industrial applications. It executes real-time speech recognition of a 60k-word dictation task on low-spec PCs with small footprint, and even on embedded devices. Julius supports standard language models such as statistical N-gram model and rule-based grammars, as well as Hidden Markov Model (HMM) as an acoustic model. One can build a speech recognition system of his own purpose, or can integrate the speech recognition capability to a variety of applications using Julius.

##### 4.2 Raspbian OS

Raspbian is Debian-based computer system for Raspberry Pi. There are several versions of Raspbian including Raspbian Stretch and Raspbian Jessie. Since 2015 it has been officially provided by the Raspberry Pi Foundation as the primary operating system for the family of Raspberry Pi single-board computers. Raspbian was created by Mike

Thompson and Peter Green as an independent project. The initial build was completed in June 2012.

The operating system is still under active development. Raspbian is highly optimized for the line's performance ARM CPUs.

#### 5. Working

An Arduino UNO controller is set to command six servo motors following instructions received by an USB connected Raspberry Pi mini-computer with the speech recognition decoder Julius. Raspberry Pi model will run the Julius program and corresponding recognized words will be forwarded to hand movement system character by character.

#### 6. CONCLUSION

We have introduced, and evaluated the feasibility of a voice to SL translator for letters and numbers with affordable open technologies (*i.e.* Arduino UNO controller and Raspberry Pi mini-computer). As far as we know, our results are the first instance of a voice-controlled robotic hand specially built with the aim to help deaf individuals. To translate automatically a spoken language into a specific SL is certainly the most challenging target since SL is mainly a visual language also incorporating complex gestures, facial expressions, head movements and body language.

#### REFERENCES

- [1] World Health Organization (WHO), 2013 Deafness and Hearing Loss Statistics, at : <http://www.who.int/mediacentre/factsheets/fs300/en>
- [2] Wikipedia on "Sign Languages relation with Spoken Languages" at : [http://en.wikipedia.org/wiki/Sign\\_language](http://en.wikipedia.org/wiki/Sign_language)
- [3] Raspberry Pi credit-card sized computer at <http://www.raspberrypi.org>
- [4] The Arduino Uno microcontroller board a <http://www.arduino.cc> Servo.h library available at : <http://arduino.cc/en/reference/servo>

**BIOGRAPHIES**

Prof S. V. Sonar  
ME in Electronics and  
Telecommunication Engineering.



Payal Das  
Pursuing BE in Electronics and  
Telecommunication Engineering,  
Konkan Gyanpeeth College of  
Engineering, Karjat.



Aaditya Ghag  
Pursuing BE in Electronics and  
Telecommunication Engineering,  
Konkan Gyanpeeth College of  
Engineering, Karjat.



Lalita Maurya  
Pursuing BE in Electronics and  
Telecommunication Engineering,  
Konkan Gyanpeeth College of  
Engineering, Karjat.

# Identifying Key Success Factors of Sustainability in Supply Chain Management for Industry 4.0 Using DEMATEL Method



Malleshappa T. Bhagawati, E. Manavalan, K. Jayakrishna and P. Venkumar

**Abstract** There is an increase in demand for industrial systems to be more competitive to expand their product reach and streamline their supply chain processes. The vision of sustainable supply chain is becoming reality as rapid advancements are happening in digital technologies. With the emerging fourth industrial revolution industry 4.0, the supply chain environment is compactly interconnected with the devices, equipment, and human that allows accessing and analyzing the real-time information. Based on the literature survey, a framework model with main perspectives and performance factors are developed to assess the sustainability of an automotive organization. Importance of performance factors and their relations are analyzed through DEMATEL technique. The result shows that Internet of Things and environment-friendly practices are the two major influential performance factors in order to become a more sustainable organization to meet industry 4.0 requirements.

**Keywords** Sustainable supply chain · Industry 4.0 · DEMATEL method

## Abbreviations

SSC	Sustainable Supply Chain
SCM	Supply Chain Management
SSCM	Sustainable Supply Chain Management
IoT	Internet of Things
CPS	Cyber-Physical System
DEMATEL	Decision-Making Trial and Evaluation Laboratory

---

M. T. Bhagawati (✉) · P. Venkumar  
Department of Mechanical Engineering, Kalasalingam University,  
Krishnankoil, Virudhunagar, Tamil Nadu, India  
e-mail: malleshbhagawati@gmail.com

E. Manavalan · K. Jayakrishna  
School of Mechanical Engineering, VIT University, Vellore, India  
e-mail: mail2jaikrish@gmail.com

© Springer Nature Singapore Pte Ltd. 2019  
H. Vasudevan et al. (eds.), *Proceedings of International Conference on Intelligent Manufacturing and Automation*, Lecture Notes in Mechanical Engineering,  
[https://doi.org/10.1007/978-981-13-2490-1\\_54](https://doi.org/10.1007/978-981-13-2490-1_54)

MCDM      Multi Criteria Decision-Making  
NIDR      Normalized Initial Direct Relation

## 1 Introduction

Organizations started bringing innovative solutions to stay ahead of the competition and transform customer expectations into reality with the help of digital technology industry 4.0 leverages digital technologies so that interaction happens among components-machines-human to bring personalized items within mass manufacturing process [1].

In this article, the investigation on perspectives and performance factors that affects sustainability of an organization has been studied in the context of industry 4.0. The objective of this research is to study the preparedness of an automotive organization to become a more sustainable organization in industry 4.0 era. The flow of the article is framed as follows. Section 2 presents the literature on industry 4.0 and sustainable performance factors. Section 3 identifies the dominant performance factors using DEMATEL method. Section 4 discusses the importance of sustainability in SCM from industry 4.0, followed by concluding remarks in Sect. 5.

## 2 Literature Review

The literature has been reviewed from different perspectives of SSCM. Based on the literature, the focus on sustainability of SCM from industry 4.0 perspective has not been reported by researchers. The study is conducted for analyzing the various perspectives of sustainable supply chain organization to meet industry 4.0 requirements. A framework model is developed for assessing sustainability in an organization as presented in Table 1. The framework has two levels. The first level contains five sustainability perspectives represented as " $P_x$ ", which influences the sustainability; the second level contains 13 sustainability performance factor represented as " $PF_x$ ".

## 3 Methodology

A model for SSC perspectives and performance factors is formulated based on the literature. An organization to carry out the case study is identified. Later, the causal relations among performance factors are analyzed using DEMATEL, and recommendations based on the relations are suggested.



**Table 1** Framework for evaluating sustainability of supply chain

Perspective ( $P_x$ )	Performance factor (PF $_x$ )
Business perspective ( $P_1$ )	Operational management (PF $_1$ ) [2]
	Supplier management (PF $_2$ ) [3]
	Strategic sourcing (PF $_3$ ) [3]
	Services management (PF $_4$ ) [4]
Technology perspective ( $P_2$ )	IoT (PF $_5$ ) [5]
	CPS (PF $_6$ ) [6]
Sustainable development perspective ( $P_3$ )	Economic (PF $_7$ ) [7]
	Social (PF $_8$ ) [8]
	Environment (PF $_9$ ) [9]
Collaboration perspective ( $P_4$ )	Logistics integration (PF $_{10}$ ) [10]
	Customer response adoption (PF $_{11}$ ) [11]
Management strategy perspective ( $P_5$ )	Cost management (PF $_{12}$ ) [12]
	Time management (PF $_{13}$ ) [12]

### 3.1 Case Study

The case study is performed in a leading automotive organization located in India (henceforth referred as ABC). ABC manufactures disk pads, brake linings, and clutch facings. ABC is the suitable organization to perform this study, as the management is optimistic and look forward in becoming a sustainable firm.

### 3.2 Use DEMATEL Method on Performance Factors

The process of DEMATEL method is summarized with the following steps [13].

*Stage 1.* Collection of feedback from subject matter specialists, and computation of average matrix

Each subject matter specialist ( $m$ ) is requested to provide the feedback as per the questionnaire prepared. The feedback received are in the scale of 0–4 where 0 implies no impact, 1 implies low impact, 2 implies moderate impact, 3 implies severe impact, and 4 implies very severe impact, respectively, denoting the effect of a factor on another factor.

For each subject matter specialist, a matrix is calculated by  $X^k = [x_{ij}^k]$ , where  $k$  represents number of participants.

Consolidating all scores from specialists ( $m$ ), average matrix  $Z = [z_{ij}]$  is mentioned as follows.

$$z_{ij} = \frac{1}{m} \sum_{k=1}^m x_{ij}^k \tag{1}$$

Stage 2. Computation of NIDR matrix ( $D$ )

A NIDR matrix,  $D = [d_{ij}]$ , wherein every constituent in the matrix is in the range of zero to one. Equation (2) is presented below.

$$D = \lambda \times Z. \tag{2}$$

where

$$\lambda = \text{Min} \left[ \frac{1}{\max_{1 \leq i \leq n} \sum_{j=1}^n |z_{ij}|}, \frac{1}{\max_{1 \leq i \leq n} \sum_{i=1}^n |z_{ij}|} \right]$$

Stage 3. Computation of influence matrix ( $T$ )

Below is the influence matrix  $T$ .

$$T = D(I - D)^{-1} \tag{3}$$

where  $I$  represents identity matrix.

Using pair-wise comparisons, scores of subject matter specialists are computed to form average matrix  $Z$  with reference to Eq. (1). The NIDR matrix  $D$  is calculated by applying Eq. (2). The overall relation matrix  $T$  is calculated with reference to Eq. (3) as illustrated in Table 2.

Stage 4. Summation of columns and rows

In this matrix, the summation of columns and rows is denoted through variables  $c$  and  $r$  correspondingly.

$$r = [r_i]_{n \times 1} = \left( \sum_{j=1}^n t_{ij} \right)_{n \times 1} \tag{4}$$

$$c = [c_j]'_{1 \times n} = \left( \sum_{j=1}^n t_{ij} \right)'_{1 \times n} \tag{5}$$

where  $[c_j]'$  is denoted as transposition matrix.

The summation of rows as well as the columns of matrix  $T$  is computed with reference to Eqs. (4) and (5) as mentioned in Table 3.

Stage 5. Computation of threshold value

**Table 2** Total influence of performance factors

	PF <sub>1</sub>	PF <sub>2</sub>	PF <sub>3</sub>	PF <sub>4</sub>	PF <sub>5</sub>	PF <sub>6</sub>	PF <sub>7</sub>	PF <sub>8</sub>	PF <sub>9</sub>	PF <sub>10</sub>	PF <sub>11</sub>	PF <sub>12</sub>	PF <sub>13</sub>
PF <sub>1</sub>	0.271	0.352	0.352	0.319	0.298	0.330	0.324	0.311	0.203	0.352	0.289	0.208	0.314
PF <sub>2</sub>	0.337	0.252	0.310	0.288	0.269	0.293	0.293	0.281	0.274	0.312	0.267	0.278	0.283
PF <sub>3</sub>	0.197	0.195	0.152	0.178	0.159	0.173	0.189	0.173	0.169	0.212	0.160	0.170	0.183
PF <sub>4</sub>	0.218	0.217	0.109	0.155	0.178	0.102	0.102	0.194	0.189	0.101	0.180	0.184	0.195
PF <sub>5</sub>	0.366	0.363	0.364	0.346	0.248	0.344	0.359	0.337	0.328	0.372	0.331	0.334	0.348
PF <sub>6</sub>	0.291	0.289	0.282	0.267	0.242	0.212	0.271	0.261	0.246	0.281	0.256	0.240	0.255
PF <sub>7</sub>	0.294	0.292	0.292	0.278	0.267	0.280	0.222	0.260	0.264	0.290	0.266	0.266	0.265
PF <sub>8</sub>	0.282	0.270	0.272	0.258	0.242	0.271	0.260	0.190	0.253	0.288	0.255	0.249	0.262
PF <sub>9</sub>	0.373	0.360	0.362	0.344	0.322	0.340	0.349	0.335	0.251	0.362	0.321	0.330	0.338
PF <sub>10</sub>	0.297	0.287	0.296	0.281	0.255	0.286	0.277	0.258	0.252	0.227	0.261	0.256	0.268
PF <sub>11</sub>	0.289	0.287	0.296	0.273	0.248	0.286	0.286	0.258	0.250	0.287	0.102	0.272	0.250
PF <sub>12</sub>	0.285	0.283	0.283	0.269	0.244	0.282	0.274	0.263	0.256	0.275	0.258	0.101	0.265
PF <sub>13</sub>	0.277	0.275	0.267	0.254	0.245	0.258	0.266	0.255	0.241	0.275	0.251	0.245	0.198

**Table 3** Results on performance factors significance

Performance factors	$r_i$	$c_i$	$r_i + c_i$	$r_i - c_i$
Operational management (PF <sub>1</sub> )	3.923	3.777	7.7	0.146
Supplier management (PF <sub>2</sub> )	3.737	3.722	7.459	0.015
Strategic sourcing (PF <sub>3</sub> )	2.31	3.637	5.947	-1.327
Services management (PF <sub>4</sub> )	2.124	3.51	5.634	-1.386
IoT (PF <sub>5</sub> )	4.44	3.217	7.657	1.223
CPS (PF <sub>6</sub> )	3.393	3.457	6.85	-0.064
Economic (PF <sub>7</sub> )	3.536	3.472	7.008	0.064
Social (PF <sub>8</sub> )	3.352	3.376	6.728	-0.024
Environment (PF <sub>9</sub> )	4.387	3.176	7.563	1.211
Logistics integration (PF <sub>10</sub> )	3.501	3.634	7.135	-0.133
Customer response adoption (PF <sub>11</sub> )	3.384	3.197	6.581	0.187
Cost management (PF <sub>12</sub> )	3.338	3.133	6.471	0.205
Time management (PF <sub>13</sub> )	3.307	3.424	6.731	-0.117

Threshold value referred as  $\alpha$  is derived as follows.

$$\alpha = \frac{\sum_{i=1}^n \sum_{j=1}^n [t_{ij}]}{N} \tag{6}$$

where  $N$  represents all number of constituent as per matrix  $T$ .

The threshold value  $\alpha$  is calculated from Eq. (6).

$$\alpha = \frac{44.732}{169} = 0.265$$

Stage 6. Construction of interrelationship graph

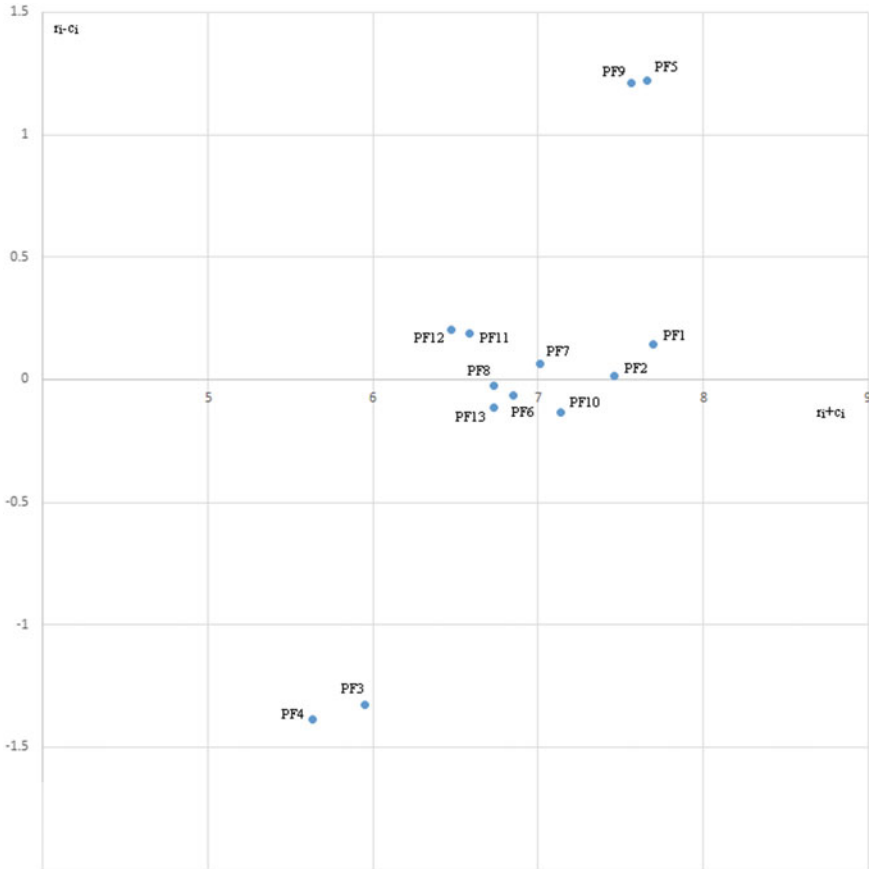


Fig. 1 Cause and effect graph for performance factors

The graph is plotted with the calculated data ( $r_i + c_i, r_i - c_i$ ) to understand the interrelationship. This graph helps to analyze the critical performance factors and understand how it influences other performance factors. The values that are greater than threshold value  $\alpha$  (0.265) in Table 2 are considered for cause and effect analysis. The dominant performance factors are IoT (PF5) and environment (PF9) from the interrelationship graph as illustrated in Fig. 1.

### 4 Results and Discussion

As illustrated in Table 3, the importance of sustainability in SCM from industry 4.0 perspective are found as  $PF_5 > PF_9 > PF_1 > PF_2 > PF_7 > PF_{10} > PF_6 > PF_{11} > PF_8 > PF_{12} > PF_{13} > PF_3 > PF_4$  with reference to performance factors importance ( $r_i + c_i$ ).

From Table 3, the major influential factors are IoT (PF<sub>5</sub>), environment (PF<sub>9</sub>), and operational management (PF<sub>1</sub>) having values 4.44, 4.387, 3.923 respectively. Similarly, the less influential factors are services management (PF<sub>4</sub>) and strategic sourcing (PF<sub>3</sub>) having the values 2.124 and 2.31 correspondingly. On discussing the findings with management, they are more interested to implement the dominant performance factors, which influence other performance factors. Management have taken few initiatives to use IoT and working on environment protection measures to move closer toward industry 4.0.

## 5 Conclusion

The future trend of supply chain will be investing in self-sustainable systems with the help of industry 4.0. The evaluated performance factors will help the organization to move toward digitalization from a sustainability perspective. A framework model has been developed with five perspectives and 13 performance factors. Using DEMATEL method, the influencing performance factors are identified, and cause and effect relationship among them are analyzed. The outcome of the analysis suggests that the management need to adopt IoT and environment-friendly practices, as these are the two most important performance factors to fulfill the industry 4.0 requirements. Focus on IoT influences the transformation of preventive to predictive maintenance and improves the overall operational efficiency. Further, emphasis on environment-friendly practices develops awareness among supply chain partners and enriches overall competitiveness and profitability.

## References

1. Cisneros-Cabrera, S., Ramzan, A., Sampaio, P., Mehandjiev, N.: Digital Marketplaces for Industry 4.0: A Survey and Gap Analysis. In Working Conference on Virtual Enterprises, Springer, Cham (2017) 18–27
2. Corbett, C.J., Kleindorfer, P.R.: Environmental management and operations management: introduction to the third special issue. *Production and Operations Management* (2003) 287–289
3. Jayaram, J., Xu, K., Nicolae, M.: The direct and contingency effects of supplier coordination and customer coordination on quality and flexibility performance. *International Journal of Production Research* (2011) 59–85
4. Balsmeier, P., Voisin, W.J.: Supply chain management: a time-based strategy. *Industrial management-Chicago then Atlanta* (1996) 24–27
5. Tu, M., Chung, W.H., Chiu, C.K., Chung, W., Tzeng, Y.: A novel IoT-based dynamic carbon footprint approach to reducing uncertainties in carbon footprint assessment of a solar PV supply chain. In *Industrial Engineering and Applications (ICIEA), 2017 4th International Conference, IEEE* (2017) 249–254
6. Monostori, L., Kádár, B., Bauernhansl, T., Kondoh, S., Kumara, S., Reinhart, G., Sauer, O., Schuh, G., Sihn, W., Ueda, K.: Cyber-physical systems in manufacturing. *CIRP Annals* (2016) 621–641

7. Genovese, A., Acquaye, AA., Figueroa, A., Koh, SL.: Sustainable supply chain management and the transition towards a circular economy: Evidence and some applications. *Omega* (2017) 344–357
8. Wu, Z., Pagell, M.: Balancing priorities: Decision-making in sustainable supply chain management. *Journal of Operations Management* (2011) 577–590
9. Andersen, MS.: An introductory note on the environmental economics of the circular economy. *Sustainability Science* (2007) 133–140
10. Qaiser, FH., Ahmed, K., Sykora, M., Choudhary, A., Simpson, M.: Decision support systems for sustainable logistics: a review and bibliometric analysis. *Industrial Management & Data Systems* (2017) 1376–1388
11. Barratt, M.: Understanding the meaning of collaboration in the supply chain. *Supply Chain Management: an international journal* (2004) 30–42
12. Um, J., Lyons, A., Lam, HK., Cheng, TC., Dominguez-Pery, C.: Product variety management and supply chain performance: A capability perspective on their relationships and competitiveness implications. *International Journal of Production Economics* (2017) 15–26
13. Sumrit, D., Anuntavoranich, P.: Using DEMATEL method to analyze the causal relations on technological innovation capability evaluation factors in Thai technology-based firms. *International Transaction Journal of Engineering, Management, & Applied Sciences & Technologies* (2013) 81–103